Impact breccia and ejecta from the Mjølnir crater in the Barents Sea - The Ragnarok Formation and Sindre Bed

Henning Dypvik, Atle Mørk, Morten Smelror, Pål T. Sandbakken, Filippos Tsikalas, Jorunn Os Vigran, Gerd Merethe A. Bremer, Jenö Nagy, Roy H. Gabrielsen, Jan Inge Faleide, Gashawbeza Mengisu Bahiru & Hermann M. Weiss

Dypvik, H., Mørk, A., Smelror, M., Sandbakken, P.T., Tsikalas, F., Vigran, J.O., Bremer, G.M.A., Nagy, J., Gabrielsen, R.H., Faleide, J.I., Bahiru, G.M. & Weiss, H.M.: Impact breccia and ejecta from the Mjølnir crater in the Barents Sea – The Ragnarok Formation and Sindre Bed. *Norwegian Journal of Geology,* vol. 84, pp. 143-167. Oslo 2004. ISSN 029-196X.

In this study we present the stratigraphic succession related to the Mjølnir impact in the Barents Sea, based on available cores, detailed sedimentological and palaeontological descriptions, as well as seismic reflection profiles. The Mjølnir impact took place in the palaeoBarents Sea, close to the Volgian - Ryazanian boundary. The epicontinental sea had a water depth of 300 - 500 m, and was characterized by anoxic to hypoxic deposition of organic rich clays, presently with kerogen of types II and I. The bolide, about 1.5 - 2.0 km in size, hit the sea/sea floor and created the 40 km wide Mjølnir crater. The Ragnarok Formation is defined as the locally derived allochthonous (mixture of re-deposited excavated material, fall back ejecta and back wash material) to parautochthonous (structurally uplifted, slumped and inverted target material from deeper levels) breccia deposits that were formed during and immediately after the Mjølnir impact. The uppermost part of the formation has been cored by a stratigraphic drilling (7329/03-U-01). It comprises siliciclastic sediments from claystones to conglomerates and consists of chaotic slump and avalanche deposits, along with different mass flow deposits. The formation is normally overlain by shales and siltstones of the uppermost part of the Hekkingen Formation (Oxfordian –Berriasian), and are succeeded by marls of the Klippfisk Formation (Berriasian-Hauterivian). On seismic reflection profiles the Ragnarok Formation can reach thicknesses of 1.3 km, including uplifted, reworked Lower Triassic fragments which originated about 3.5 km down in the crust and were structurally elevated during the impact cratering stage. The Ragnarok Formation reaches its maximum thickness in a wedge-shaped annular trough beneath the present annular crater basin, pinching out both towards the crater centre and towards the periphery. It can be recognised in seismic reflection profiles at the Mjølnir crater location and up to ~55 km away from the crater centre, forming a wedge-shaped unit within the Mesozoic siliciclastic deposits of the Bjarmeland Platform. During the oblique Mjølnir impact event, large amounts of material were ejected and widely dispersed. Models of the impact process suggest that the ejecta were mainly spread in a north-easterly direction. The impact-related ejecta bed outside the crater boundaries varies from millimetres to a few metres in thickness and has been named the Sindre Bed. It has been recognized in core 7430/10-U-01, and in other wells of the Barents Sea. An Ir-enrichment in a time-equivalent formation at Nordvik, North Central Siberia, possibly represents a distal variety of the Sindre Bed.

Henning Dypvik, Filippos Tsikalas, G. Merethe A. Bremer, Jenö Nagy and Jan Inge Faleide, University of Oslo, Department of Geosciences, P.O. Box 1047 Blindern, NO-0316 Oslo, Norway; Atle Mørk and Hermann M. Weiss, SINTEF Petroleum Research, NO-7465 Trondheim, Norway; Morten Smelror, Geological Survey of Norway, NO-7491 Trondheim, Norway; Pål T. Sandbakken, Statoil ASA, NO-4035 Stavanger, Norway; Jorunn O. Vigran, Mellomila 2, NO-7018 Trondheim, Norway; Roy H.Gabrielsen, Norges Forskningsråd, P.O. Box 2700, St.Hanshaugen, NO-0131 Oslo, Norway; Gashawbeza Mengistu Bahiru, Geological Survey of Ethiopia, P.O. Box 2302, Addis Abeba, Ethiopia.

Introduction

Impact craters can generally be divided into two main categories: simple bowl-shaped and complex craters with central peaks and peak rings. The impact process can theoretically be subdivided into three main stages (Melosh 1989; French 1998). During the first two stages, compression and excavation, the rocks and sediments in the target area are compressed and crushed, partly melted and evaporated, and large amounts may be ejected. During the following modification stage, the crater is modified by various processes. In submarine impacts resurge activity along with slides, slumps, avalanches and gravity flows from the crater rims, peak rings and central peaks of the basin often represent the first part of the modification stage of the impact. Modification of the crater and sediments in the area, however, continues until the present day. The crater rim, central peak and peak rings will be levelled out, and much of this material will eventually be deposited in the various sub-basins of the crater, contemporaneously with the regular background sedimentation in the area.

The Mjølnir crater is a well-established marine impact complex crater, 40 km in diameter, located on the Bjarmeland Platform in the central Barents Sea (Fig. 1) (Gudlaugsson 1993; Dypvik et al. 1996; Tsikalas et al. 1999). Both geophysical and geological data unequivocally substantiate an impact of a meteoritic bolide 1 - 3 km in diameter at ~142 Ma into an epicontinental

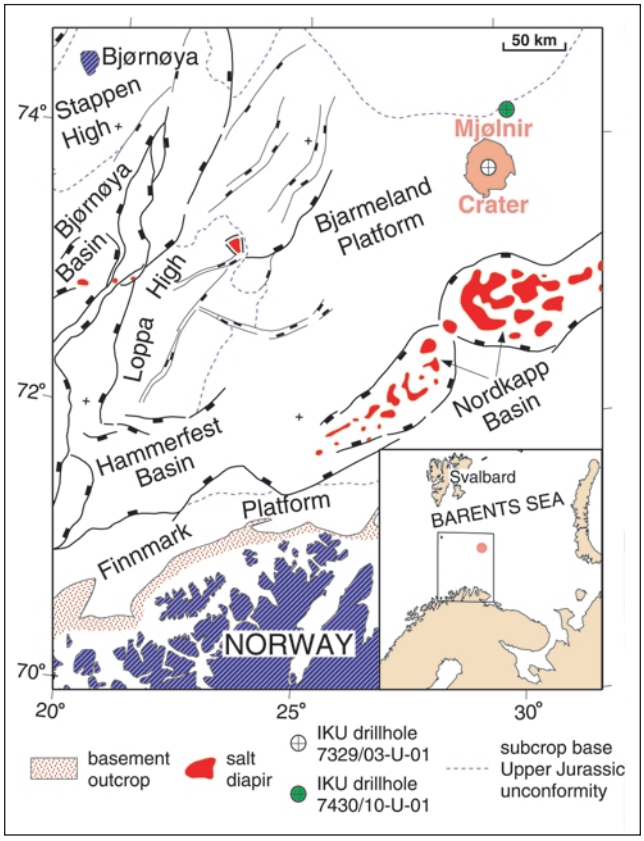

Fig. 1. Location of the 40 km diameter Mjølnir crater relative to the main Late Jurassic-Early Cretaceous structural elements in the southwestern Barents Sea, showing the location of the two shallow drillholes used in this study (from Tsikalas et al. 1998b).

basin with 300 - 500 m palaeo-water depth (Gudlaugsson 1993; Dypvik et al. 1996; Smelror et al. 2001; Tsikalas et al. 2002a). A total of ~2100 km of seismic reflection profiles clearly image the impact-related and post-impact structure and stratigraphy (Fig. 2). In addition, free-air gravity and seismic velocity anomalies exhibit a close correspondence to the impact-induced structure and the spatial distribution of physical properties (Tsikalas et al. 1998a-c). Two shallow boreholes, one near the crater centre (Mjølnir core 7329/03-U-01) and another ~30 km from the crater periphery (7430/10-U-01) (Fig. 1) have confirmed the impact origin of the structure and permit a detailed seismic stratigraphic correlation to be made (Tsikalas et al. 2002a). The cores from the holes reveal brecciated sediments containing shocked quartz grains, showing a zonation with abundant planar fractures and planar deformation features, and a prominent ejecta layer with strong iridium enrichment (Dypvik et al. 1996; Dypvik & Ferrell 1998; Dypvik & Attrep 1999; Sandbakken 2002).

At the time of impact, the Barents Platform consisted of Upper Palaeozoic strata, mainly carbonates and evaporites, overlain by 3 - 4 km thick Mesozoic siliciclastic marine sediments (Fig. 3). The Mjølnir impact resulted in an extensive disturbance of both the water column and the sediments in the target area, which led to the formation of an array of structural features on the seabed and deep into the targeted rocks. The energy released during the Mjølnir impact is directly related to the volume of ejected material and to tsunami generation. These processes affected both the Barents Sea region and adjacent areas in the Arctic (Shuvalov et al. 2002; Shuvalov & Dypvik 2004).

Recent studies of marine target impacts and systematic compilations of their structural and morphological features have shown that there are significant differences between impact craters formed on land and those at sea (Gersonde & Deutsch 2000; Ormö & Lindström 2000; Dypvik & Jansa 2003; Dypvik et al. 2004a). The primary cause for several of these differences is the water content of the sediments and the overlying sea water. These fatures trigger various erosional and depositional processes that do not occur on land. During a marine impact, the growing crater rim and the ejecta curtain push the water outwards forming a water cavity. Collapse of this water cavity starts at its base and causes a water flow towards the crater (Shuvalov 2002). When the water depth is sufficient to overflow and cut through any uplifted rim, characteristic erosional/-depositional resurge gullies can be formed, acting as inlets for water and for material flowing back into the crater. This flow greatly affects the crater rim and leads to extensive infilling, in addition to slumping, slides, avalanches and density currents formed by the collapsing, water-saturated sediments of the rim, the peak rings and the central high. These complex sedimentation processes mix sediments of variable lithologies and stratigraphical levels, representing major parts of the Mesozoic succession of the impact area. A relatively detailed description of these rocks is given below.

The detailed sedimentology and petrography of the sediments associated with the Mjølnir impact event have earlier been presented in several papers (e.g. Dypvik & Attrep 1999; Dypvik et al. 2003, 2004b). In the present paper we define the main stratigraphical units and discuss their formation and stratigraphical importance.

The geology of the Barents Sea and Svalbard areas

The present sea floor of the Barents Shelf was sculptured during and after the last glaciation, with underlying Cenozoic, Mesozoic and Upper Palaeozoic sediments resting on a Caledonian basement.

An extensive programme of seismic investigations on the southern part of the Barents Sea has been carried out for hydrocarbon exploration. Sixty-one exploration wells have been drilled in the Norwegian sector of the

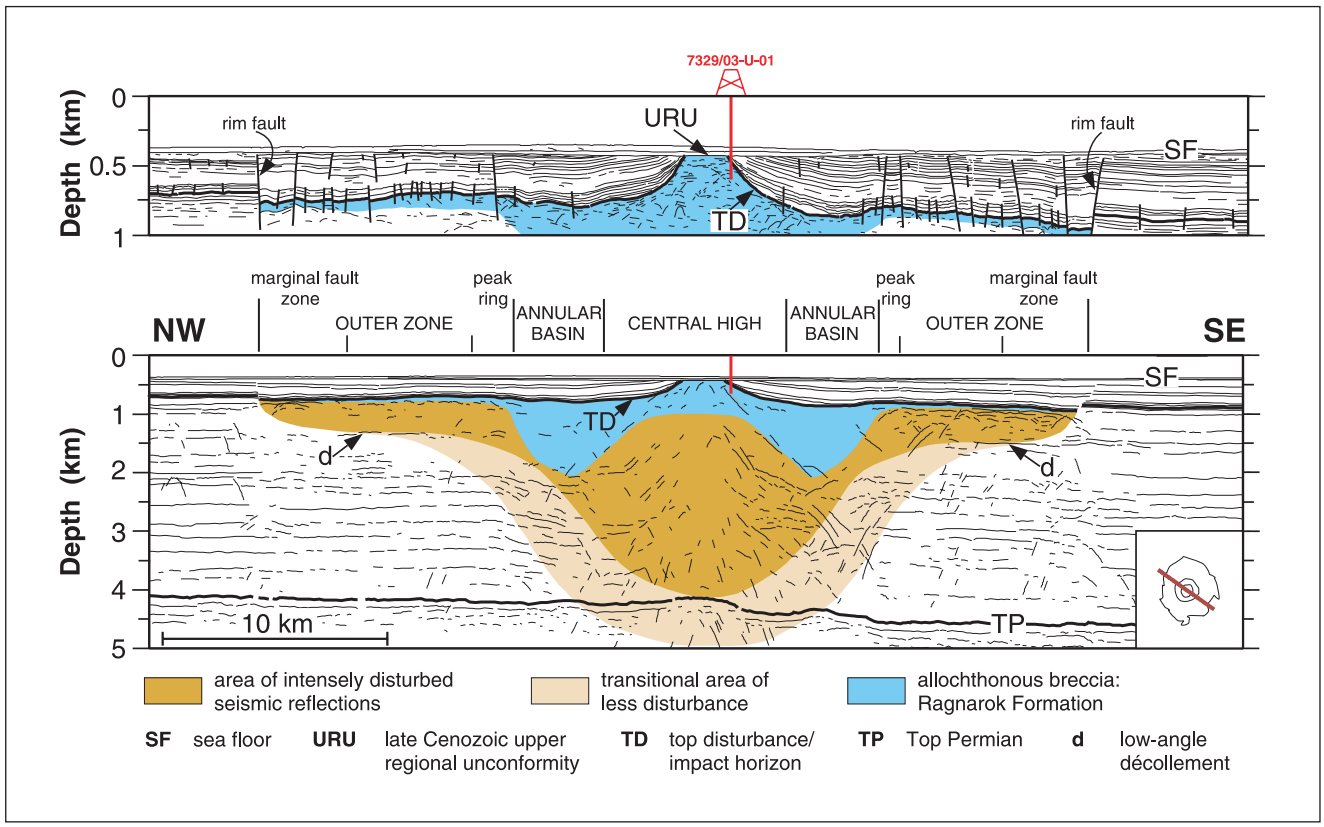

Fig. 2a. Seismic type sections. Top: Interpreted high-resolution single-channel profile. Bottom: Interpreted multi-channel profile (from Tsikalas et al. 1998a, c).

sea (NPD website, URL in reference list) and a somewhat lesser number on the Russian side. In addition 50 shallow stratigraphic boreholes of 1 - 300 m depth have been drilled in the Norwegian part for scientific and exploration purposes.

The Barents Shelf is composed of basins, highs and platforms that were active in different geological times (Gabrielsen et al. 1990; Johansen et al. 1992). On the Russian side, the South Barents Basin and North Barents Basin are the major depocentres, while the Nordkapp, Hammerfest and Bjørnøya basins are found on the Norwegian side. Pronounced highs, such as the Central Barents High and the Bjarmeland Platform, separate these basins (Fig.1).

The stratigraphy of the Palaeozoic succession of the Svalbard archipelago has been revised by Dallmann et al. (1999) and the part of the succession in the Norwegian part of the Barents Sea by Larssen et al. (2002). Devonian and Carboniferous siliciclastic rocks represent fluvial and lacustrine sediments, partly deposited in rift basins. A change to carbonate deposition in shelf and reef environments took place in the Middle Carboniferous, followed by evaporite deposition in the Early Permian. As the region ceased to be a carbonate province, siliciclastics were deposited, but still including some carbonates of cooler and deeper water affinities. The Permian succession is rich in silica that

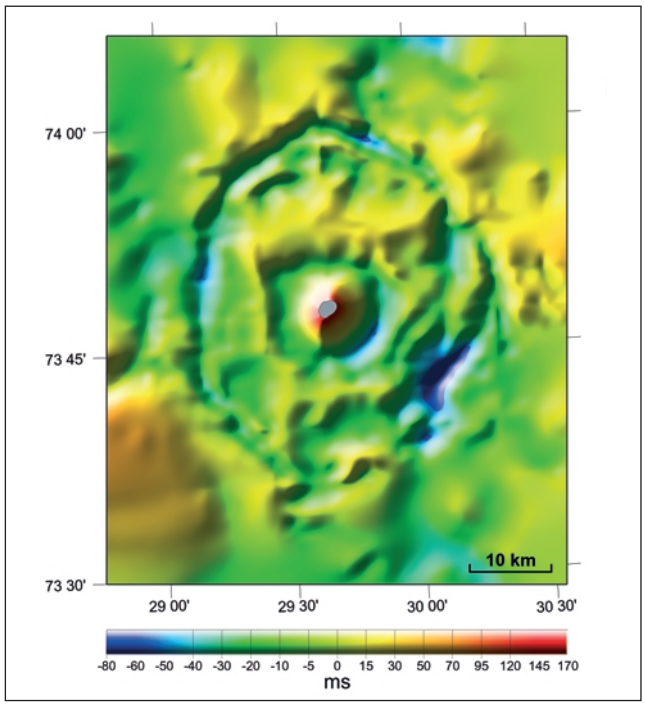

Fig. 2b. Illuminated perspective image of the present structural morphology of the Mjølnir crater approximately at the level of the impact horizon (cf. Fig. 2a), based on the entire (2127 km) seismic reflection database available. The view is directly from above; light sources are at azimuths 30º, 290º, and 340º. The grey area on top of the central high shows truncation by erosion. Vertical exaggeration ~20x (from Tsikalas et al. 1998c).

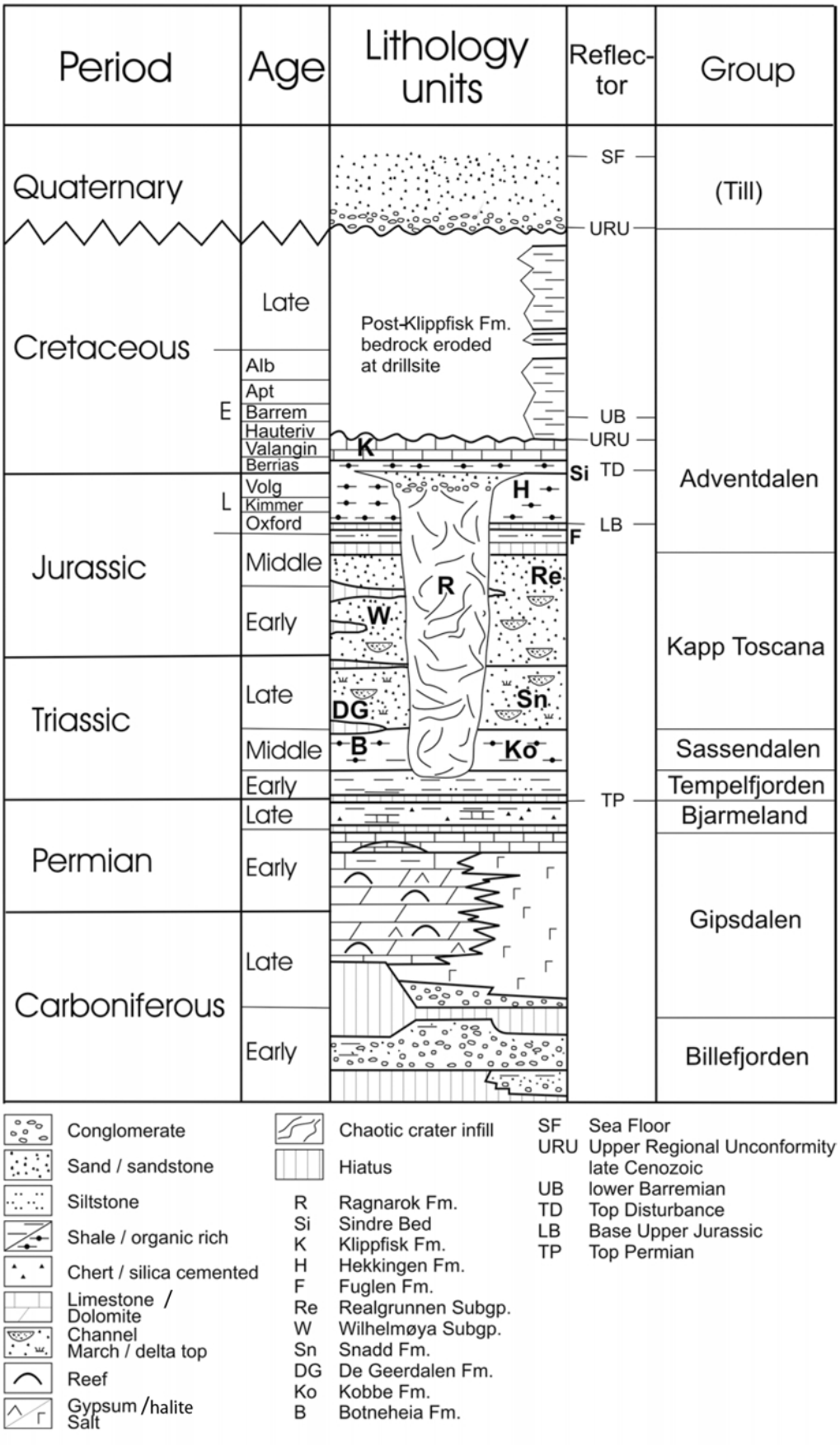

Fig. 3. General stratigraphy of the Bjarmeland Platform with the Mjølnir crater filled with the Ragnarok Formation. Lithostratigraphical units of the Bjarmeland Platform are indicated to the right of the crater, while units occurring on Svalbard are indicated to the left. Note that the impact disturbed beds down into the upper Lower Triassic, while the crater is directly overlain by lowermost Cretaceous sediments of the Hekkingen Formation.

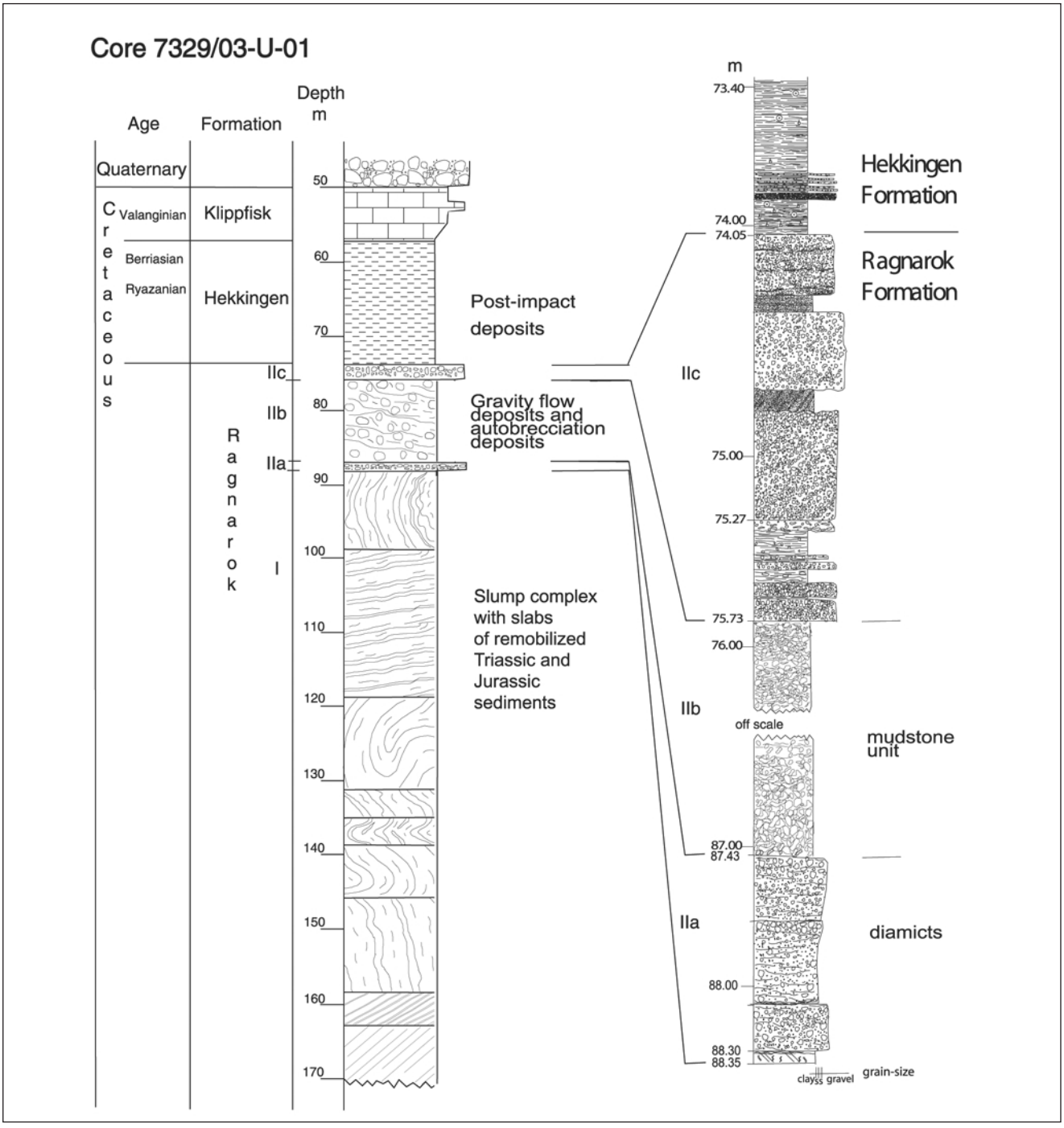

Fig. 4. General core log of 7329/03-U-01 (left) and log through Units I and II (right) is shown. Details of these units are shown in Figs. 6, 7 and 8, and core photos are displayed in Figs. 5 and 9. Modified from Dypvik et al., 2004b.

originated mainly from sponges. This resulted in a pronounced reflector marking the top of the Permian succession over the whole Barents Sea. This seismic reflector and the underlying succession were not disturbed by the Mjølnir impact (Figs. 2 and 3).

The Barents Sea succession, from durable Palaeozoic rocks to much softer shales and friable sandstones of the Mesozoic, shows a pronounced shift in the style of sedimentation. Based on well information and seismic data, Worsley et al. (1988) established the first stratigraphic subdivision of the Mesozoic succession. This subdivision is now emended and correlated with the stratigraphy of Svalbard to give a coherent scheme for the whole Norwegian Barents Shelf (Mørk et al. 1999). Shales and minor sandstone units dominate the Lower and Middle Triassic Sassendalen Group of Svalbard and the Barents Shelf (Mørk et al. 1982, 1992; Van Veen et al. 1992) (Fig. 3). Excellent hydrocarbon source rocks were deposited in a large embayment that extended from central Svalbard through the central part of the Barents Sea and turned south-westwards between Nor-

way and Greenland. Deposition of organic-rich sediments started during the Spathian in the Svalis Dome area in the central Barents Sea (Leith et al. 1992), but is extensively developed on the main Svalbard islands (Mørk & Bjorøy 1984). One peculiarity of these sediments is the occurrence of large specimens of *Tasmanites* algae, mostly several hundred micrometres in diameter, which occur abundantly in some beds (Vigran et al. 1998). Phosphate nodules are also abundant in the organic-rich shales (Mørk et al. 1982; Mørk & Bjorøy 1984; Krajewski 2000).

The sandstone-dominated Upper Triassic to Middle Jurassic Kapp Toscana Group is widely distributed in the Svalbard archipelago and the Barents Shelf (Mørk et al. 1999). The group comprises sediments deposited in shallow shelf, deltaic and paralic environments (Mørk et al. 1982, 1999). On Spitsbergen the group contains grey shales with abundant thin siderite beds representing prodelta environments of the Tschermakfjellet Formation. This unit grades into the overlying sandstones and shales of the De Geerdalen Formation. On Spitsbergen shallow marine sandstone bodies dominate, while on the eastern islands (Edgeøya, Barentsøya and Hopen) deltaic channels form stacked sandstone bodies, each several tens of metres thick. Minor coal beds are also present. This formation grades laterally into the deltaic sediments of the Snadd Formation of the Barents Sea. The Bjarmeland Platform and the areas further north also include mixed delta plain sediments consisting of fine-grained grey sandstones, abundant conglomerates, thin beds of siderite and occasional coal beds. Grey, greenish-grey to dark grey shales are also abundant.

The uppermost Triassic and Lower to Middle Jurassic part of the Kapp Toscana Group is represented by the Wilhelmøya Subgroup on Svalbard, which grades into the Realgrunnen Subgroup as defined in the southern Barents Sea (Mørk et al. 1999). Both subgroups consist of dominantly shallow marine reworked sandstones with subordinate shales and coals (Johannessen & Embry 1979; Mørk et al. 1999). The sandstones are more mineralogically mature than in formations below (Mørk 1999). The upper part of these units consists of several hiatuses and remanié conglomerates of regional extent.

A change in sedimentation regime took place in the late Middle Jurassic. On Svalbard, a basal sandstone unit grades upwards into dark shales of the Agardhfjellet Formation (Dypvik et al. 1991a, 1991b), while in the southern part of the Barents Sea a similar development is apparent in the siltstones and sandstones of the Fuglen Formation. In central parts of the Barents Sea the coarser grained unit is thin or missing, and the interval is mainly represented by the dark, organic-rich shales of the Hekkingen Formation (Mørk et al. 1999). The Hekkingen Formation normally displays very high gamma values in the lower Alge Member, while the upper Krill Member has lower gamma readings and reduced organic carbon contents (Worsley et al. 1988).

Fig 5. Photographs of key lithologies from the Mjølnir core. The core sections are 5.4 cm wide and 34 cm long. Numbers refer to the depth (in metres below seabed) at the top of each core segment. The lengthwise cut core-pieces have been mounted on perforated aluminium trays.

53.29: Marl (light greenish grey) of the Klippfisk Formation with abundant shell (Inoceramus) fragments (white). 66.38: Finely laminated, dark organic rich shale of the Hekkingen Formation with crushed shells of Buchia and ammonites (white). 74.41 and 75.02: Diamict (upper 2/3 of 74.41) and conglomerates with interbedded shales of unit IIc of the Ragnarok Formation. Note the clasts with oxidised rims in the section at 75.02 m.

The remaining photos are from Unit I of the Ragnarok Formation. 96.09 m: Folded and mixed sandstone and siltstone with spotted brownish oxidation surfaces. 108.50 m: Obliquely and disturbed siltstone and sandstone overlain at the top by a calcite cemented sandstone. Along the upper and lower bedding planes possible loading structures are evident. 110.10 m: Flat bedded, folded and faulted mixture of sandstone, siltstone and mudstone with some beds fragmented to form small clasts. 129.09 m: Strongly folded and contorted mudstone and sandstone. 134.66 m: Extremely folded, partly faulted and fluidised sandstone and mudstone beds. 142.51 m: Laminated, disturbed mudstone laminae with contorted clasts (broken laminae) of sandstones. 150.38 m: Calcite cemented sandstone overlain by mudstone with sandstone clasts. 151.11 m: Fluidised mixture of sandstone and mudstone. 156.26 m: Zig-zag folded and micro-faulted sandstone. 161.64 m: Obliquely folded siderite conglomerate overlain by well sorted calcite cemented sandstone. 162.20 m: ?Bioturbated siltstone overlain by folded siltstone and mudstone. 169.32 m: Dark grey mudstone, slightly folded.

The Jurassic - Cretaceous boundary is marked by a pronounced hiatus throughout the Barents Shelf region. On Svalbard black shales of the Rurikfjellet Formation overly the unconformity, while calcareous shales of the Knurr Formation (Valanginian - Barremian) occur at corresponding levels in the basins of the Barents Sea. On palaeo-highs like the Bjarmeland Platform, a thin (about 9 m thick) condensed carbonate marl unit is defined as the Klippfisk Formation (Berriasian - Hauterivian) (Smelror et al. 1998). The unit is greenish, white to light grey and consists mainly of marly shale and limestones with the bivalve *Inoceramus*. This unit forms the upper part of the sedimentary succession that crops out beneath the Quaternary cover in the central part of the Bjarmeland Platform. The Klippfisk Formation is overlain by dark shales of the Kolje Formation outside the most elevated areas (Mørk et al. 1999).

The Mjølnir core (7329/03-U-01)

A shallow borehole (7329/03-U-01) was drilled into the Mjølnir crater at a water depth of 350 metres in late August 1998 by the drillship M/S Bucentaur. A soil-drilling pipe was used to penetrate the 50 m thick

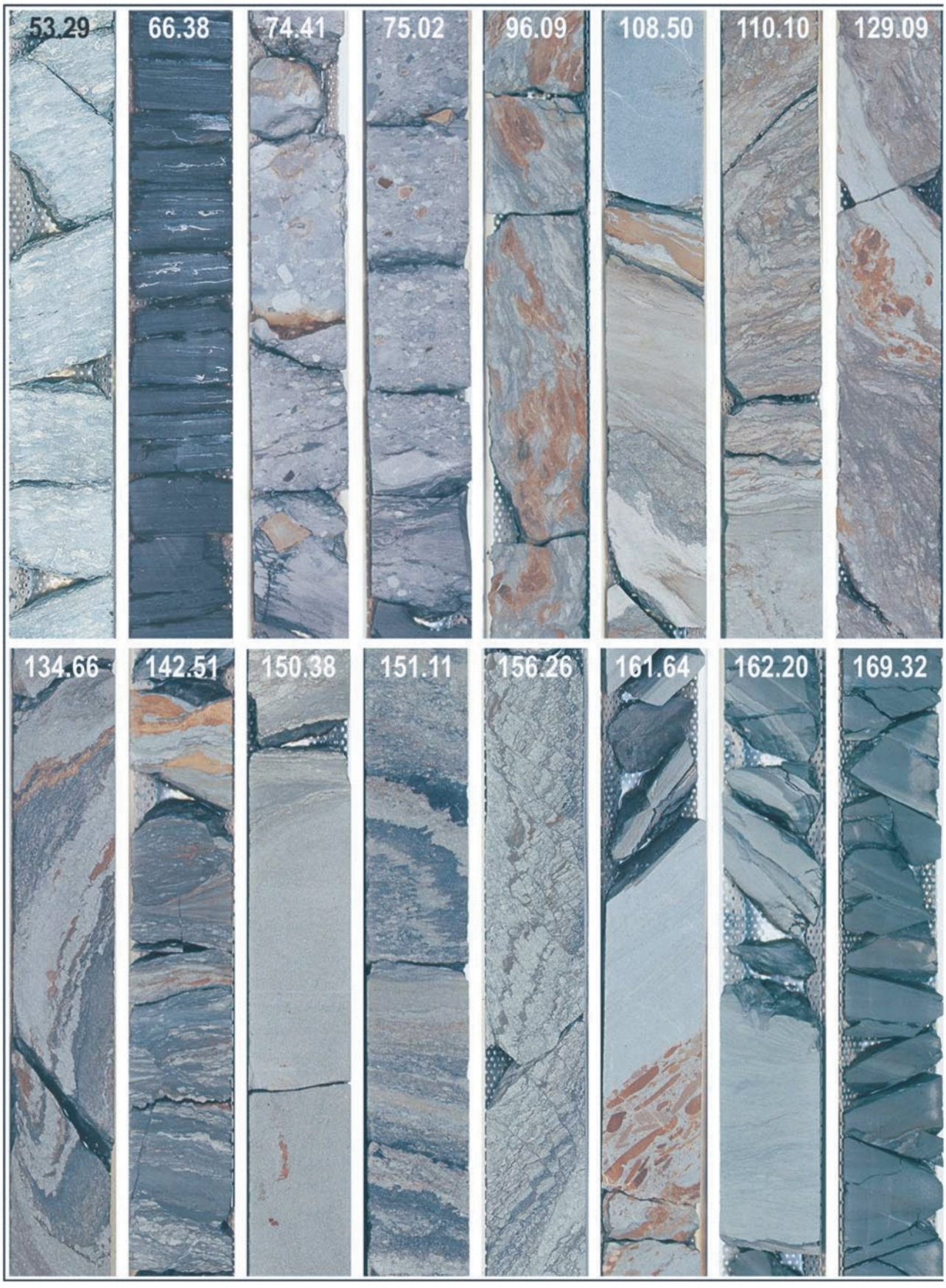
53.29
66.38
74.41
75.02
96.09
108.50
110.10
129.09
134.66
142.51
150.38
151.11
156.26
161.64
162.20
169.32

Quaternary sediment package including till (Figs. 2 and 3), but no samples were taken. An ordinary diamond drilling system placed inside the soil drilling pipe was used to core the bedrock. After every three metres of drilling, the core was retrieved using a wire-line system, then carefully extracted from the core barrel and a preliminary description made. Sonic velocity measurements and spectral gamma radiation analyses on the core were carried out where possible.

The coring operation went smoothly. The first 7 m of the marly limestones of the Klippfisk Formation were sampled, followed by 17 m of the grey, laminated shales of the Hekkingen Formation (Table 1 and Figs. 4 and 5). The rocks retrieved between 74.05 m below the seabed and the core base at 171 m differed from anything else drilled in the Barents Sea. The core had very low internal strength and pieces could not be lifted out of the core barrel without falling apart. The sound velocity could therefore not be measured regularly and only very low values were obtained, except in a few, well-cemented intervals. The lack of strength prevented measurements of natural gamma activity whilst aboard ship, and a technical breakdown that terminated the drilling operation made logging of the hole by ordinary petrophysical wireline tools impossible.

After the core had been transported to the laboratory and had been allowed to dry slowly, about 62 m had sufficient strength to be slabbed, and the parts mounted on alumina trays as display cuts (Figs. 5 - 9). The macrofossils, mainly from the Hekkingen Formation, were carefully extracted. A spectral gamma log was recorded four years after drilling, using laboratory analyses directly on the core (Figs. 10 and 11). Samples for palynological and micropaleontological analyses were extracted (Fig. 12).

The Ragnarok Formation

The disturbed rocks cored between 171 m and 74.05 m in hole 7329/03-U-01 form a map-able unit recognised within the Mjølnir crater. The occurrences of this unit are diagrammatically displayed in Fig. 3. It consists of chaotic and slump-dominated sediments (unit I) overlain by avalanche and mass- and gravity-flow deposits (unit II) (Figs. 4 and 5). The succession contains lithologies and rock fragments resembling rocks found in surrounding areas of the Barents Shelf and on Svalbard.

We suggest this unit to be called the Ragnarok Formation, to continue the mythological style of nomenclature. In Nordic mythology Mjølnir is the hammer of the god Tor, who was responsible for making thunder and lightning. Tor threw the hammer as a projectile, at items he wished to destroy. Ragnarok means Armageddon or a catastrophe with devastating consequences, such as the complete collapse of the Earth. Although the Mjølnir impact was not of such a magnitude, the name seems well suited for the chaotic sediments as they characterise the violent processes that led to their deposition. The name Ragnarok Formation had been used informally for a couple of years and was formally acknowledged as the name of the crater infill material by the Norwegian Committee on Stratigraphy in 2004. Both the Ragnarok Formation and its lateral extension, named the Sindre Bed (defined below), are included within the Adventdalen Group of Mørk et al. (1999).

The present core only penetrates the uppermost part (96.95 m) of the Ragnarok Formation (Table 1). The base of the unit is defined by seismic data. We suggest to define its lower boundary between the so-called autochthonous and allochthonous to parautochthonous breccias, extending to a depth of 1.3 km depth below sea bed (Tsikalas et al. 1998a). This level represents a recognisable horizon on seismic profiles. The Ragnarok Formation consequently includes part of the structurally uplifted and slump-back deposits (parautochthonous breccias) and the fall-out/back and reworked/retransported deposits (allochthonous breccias), while the in situ and highly fragmented brecciated rocks formed during the excavation and modification stages in the transient crater, the so-called autochthonous breccias, are found below. The Ragnarok Formation is succeeded by the Hekkingen and Klippfisk formations below a 50 m thick Quaternary cover.

The Ragnarok Formation was formed during Late Volgian - Ryazanian (Boreal Berriasian) times based on dating of the underlying and overlying sediments (Smelror et al. 2001; Bremer et al. 2003; Smelror & Dypvik in press). The formation, however, carries re-sedimented fragments, dominantly of late Early to Late Triassic and to a lesser extent of Jurassic age (see below).

Outside the Mjølnir crater rim, equivalents to the Ragnarok Formation are indicated from seismic analyses. There the Hekkingen Formation is found above and below the Ragnarok Formation. The boundaries of this wedge in these near crater areas have so far not been cored or sampled. The Sindre Bed is defined (see below) as the lateral extension of the Ragnarok Formation, representing the impact-related ejecta material outside the crater boundaries.

Ragnarok Formation, unit I

Unit I (171 - 88.35 m) (Tables 1 and 2, Figures 4 and 5) consists of strongly folded and fractured clay-, silt- and sandstones. The palynomorph assemblages comprise a mixture of taxa derived from deposits of Spathian (late Early Triassic) to Late Jurassic age (see below, Figure 12). The occasionally dominant *Botryococcus* (156.2 m) records algal growth in sediments from shallow (brackish to marine) areas.

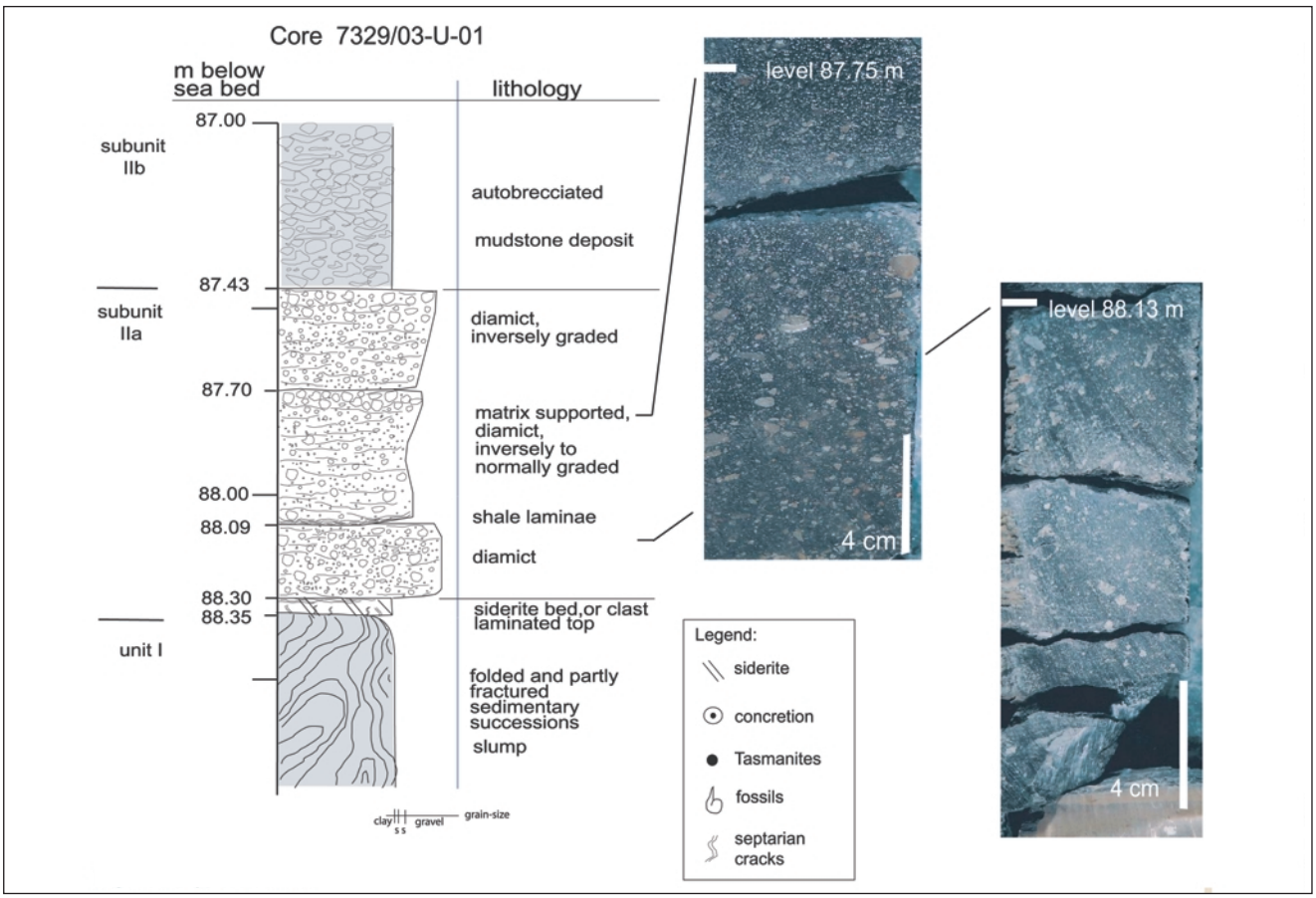

Fig. 6. Detailed core log of subunit IIa of the Ragnarok Formation from core 7329/03-U-01 and photos of some key lithologies. Modified from Dypvik et al.(2004b).

The degree of folding and faulting varies throughout the core and in some parts both vertical and horizontal bedding are found, often in combination with soft sedimentary deformation and water escape structures. Unit I has, by Dypvik et al. (2004b), been interpreted to represent reworked, folded and fractured pre-impact sediments which were deposited as scree, avalanches and slumps along the central peak of the crater.

The uppermost 120 cm of unit I contain a fragmented, brecciated bed (89.55 - 88.35 m), that has a sharp upper boundary and an angular unconformity with the overlying siderite layer (Figs. 4 and 6) and the succeeding diamict of unit IIa. This 120 cm thick bed consists of partly folded clay clasts, grain-supported in a clayey matrix. The palynomorphs show the same time span as for the deposits below (Fig. 12). Lithologically, the clasts are similar to those just below this top part, dominated by grey claystones with a low content of silt and sand.

Ragnarok Formation, unit II

Unit II (88.35 - 74.05 m) generally consists of poorly sorted conglomerates and can be divided into three subunits IIa, IIb and IIc (Figs. 4 - 8; Tables 1 and 2).

Subunit IIa consists of two well-defined parts: A lower, light brown, dense siderite bed or concretion of 5 cm thickness (88.35 - 88.30 m) and an upper 87 cm thick (88.30 - 87.43 m) diamict with a dark grey, sandy clay matrix (Table 1 and Figs. 4, 5 and 6). The siderite bed has a light brown colour (Figs. 4 and 6). Septarian cracks are typically found in the lower 3.5 cm thick section of the siderite bed. The upper 1.5 cm of the siderite bed shows a faint parallel lamination and is sharply separated from the overlying conglomerates, but shows similar bedding orientation. The cored siderite may represent a siderite concretion, but the bedding being similar to the overlying sediments indicates a possible in situ origin associated with the diamict above.

The major part (87 cm) of unit IIa is a homogeneous and poorly sorted diamict composed of a matrix-supported, dark grey, pebbly mudstone with subrounded to subangular clasts (Fig. 6). The intraclasts consist of sandy silt and claystone fragments up to about 2 cm in size, but with 2 mm as an average. The lithological compositions of the clasts resemble the reworked Triassic and Jurassic sediments also found in unit I (Figs. 5 and 6). Only faint clast-orientation has been observed in the pebbly mudstone (diamict). In Figure 6 the clasts seem to have their long parallel and horizontally orientated, indicating some shear

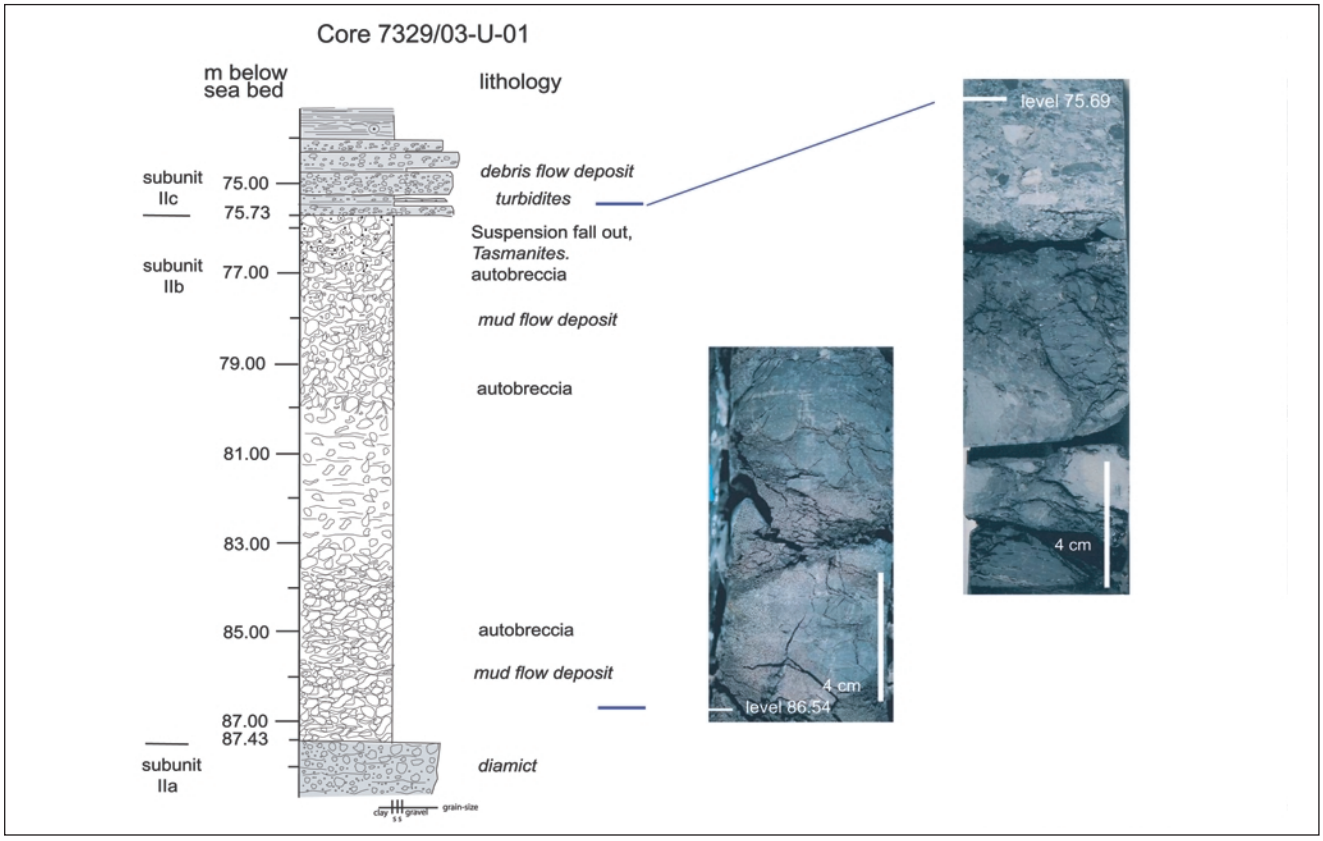

Fig. 7. Detailed core log and core photos of subunit IIb of the Ragnarok Formation. Modified from Dypvik et al. (2004b).

movement. Glass or glass fragments have not been found so far. The sediment is poorly cemented and disintegrates easily in water, as does most of unit II.

The pebbly mudstones of unit IIa may be further subdivided into three minor parts that are separated by two cm-thick layers containing irregular shear laminae. The lowermost layer (88.30 - 88.09 m) is fairly homogeneous. The overlying section (88.09 - 87.70 m) shows faint layering and contains more lightly coloured, subrounded clasts especially in its upper part (87.85 - 87.70 m). This change in colour and roundness may reflect an additional input from a different as yet unknown source. The uppermost section (87.68 - 87.43 m) shows some clast enrichments along its uppermost layers, but no changes in clast size.

In the upper part of subunit IIa, the alga *Leiosphaeridia* is present in great abundance, as is also the case in the overlying Hekkingen Formation (Bremer et al. 2003). An algal bloom of *Leiosphaeridia* is also recorded in other correlative sediments and is attributed to increased nutrition from the seawater following the impact (Smelror et al. 2002). Since recent algal blooms need weeks to develop, this may indicate that the finest grained, gravity deposited material of this subunit was deposited some time after the impact.

Subunit IIa was most likely deposited from debris or mud flows along the central peak, while the siderite bed may represent a diagenetic alteration product (Dypvik et al. 2004b). These authors claim that unit IIa represents the first collapse phase of the central peak, possibly tsunami related.

Subunit IIb (87.43 - 75.73 m) is a 11.70 m thick, homogeneous unit consisting of dark grey to brown and olive green, highly fragmented claystones (Figs. 4 - 7). A few cm-sized siderite concretions are also present. The clast- and matrix-supported unit IIb displays clay clasts in a matrix of mud. The clay clasts are composed of similar material to the matrix and are hard to distinguish macroscopically, but are easily distinguished in thin section by a more consolidated appearance than the matrix. The angular to subrounded clay clasts range in size from a few millimetres to 5 cm, indicating that the clay must have been somewhat compacted/consolidated before reworking.

The disintegrated clay clasts and matrix together consist of more than 90 % coarse clay and fine silt, with average grain sizes between 3 and 13 μm (Dypvik et al. 2004b). In the uppermost parts of the unit indications of bimodal grain size distribution are seen, with minor enrichments at 40 - 50 μm grain size. The grain-size distribution in unit IIb can generally be characterised as unimodal with a slightly fining tendency upwards. The subunit does not show any obvious bedding, except for a faintly laminated and apparently almost clast-free interval between 83 and

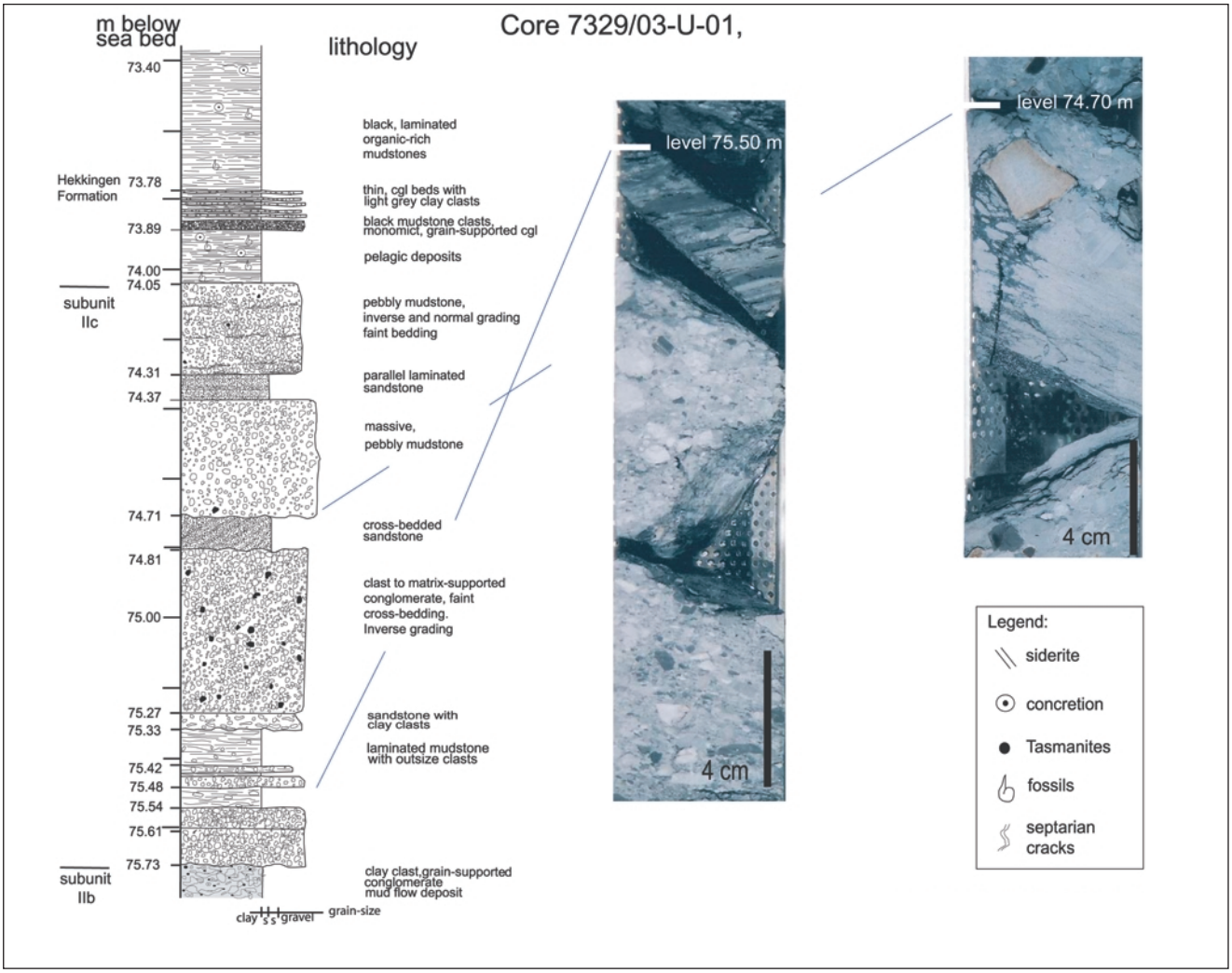

Fig. 8. Detailed core log of subunit IIc of the Ragnarok Formation and typical section photos of the Mjølnir core. Two core sections of this subunit are also displayed in Figure 5. Dark spots in conglomerates around level 75 represent mud clasts. Modified from Dypvik et al. (2004b).

81 m (Fig. 7). At a few levels, e.g. at 79.4 m, chemical alteration structures are seen as somewhat lighter bands that cut the core. Brownish alteration bands and spots are found sporadically, and are most likely secondary diagenetic feature.

Recycled palynomorphs from the subunit are of mixed Early Triassic (Spathian) to Jurassic age (Fig. 12). In the uppermost 2.5 m of subunit IIb, the prasinophyte alga *Tasmanites* is found together with 1 to 3 cm large pyrite concretions. *Tasmanites* occurs as black spheres about 0.5 mm in size. In thin sections they have a well-defined orange (light) to green appearance under crossed polars. *Tasmanites* algae of similar size are abundant in Middle Triassic sediments on Svalbard and in Northern Barents Sea cores (pers. obs. A.Mørk and J.O.Vigran).

Subunit IIb, according to Dypvik et al. (2004b), most likely represents mud-flow deposits formed by auto-brecciation in relation to tsunami reworking before the major modification phase of the crater. The upper boundary towards subunit IIc is a sharp, well-defined erosional surface which may have been caused by the succeeding density flows of subunit IIc (Figs. 7 and 8) (Dypvik et al. 2004b).

Subunit IIc (75.73 - 74.05 m) has a composition characterised by well-defined diamict, conglomerates and minor sandstone beds (Figs. 4, 5 and 8, Table 1). The three thickest conglomerate beds are composed mainly of dispersed subangular to subrounded clasts (Figs. 5 and 8). These clasts in thin section are seen to be composed predominantely of greyish dark brown clay- and siltstone with few sandstone clasts. The texture is most commonly grain-supported with a poorly sorted grey, silty to clayey sandy matrix with a few dispersed *Tasmanites* algae. Sorting is poor to moderate and clasts are distributed throughout the bed, whereas grain support increases near the top. The clasts are commonly around 3 mm in size and mainly random oriented. The largest clast found was a 4 cm long sandstone pebble. Rare brown coloured sandstone clasts show light greyish-brown coloured alteration rims, whereas no comparable rim has been observed in the much more common grey clasts (Figs. 5 and 8).

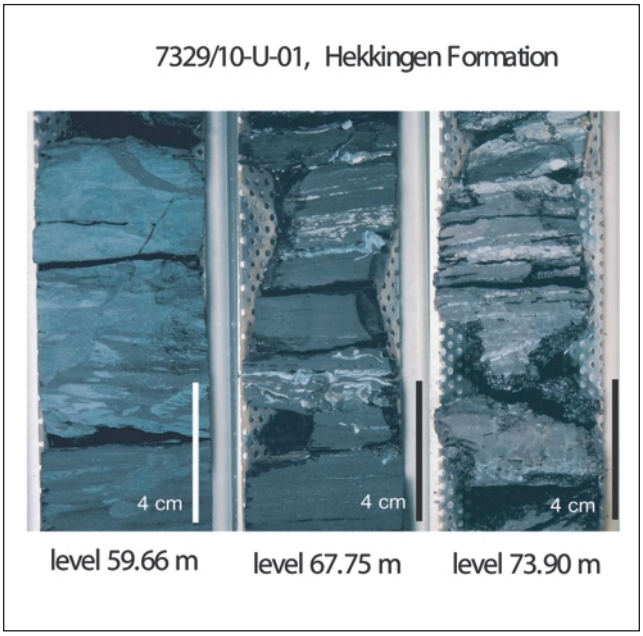

Fig. 9. Three typical developments of the Hekkingen Formation in core 7329/03-U-01. Right: Dark grey shale with coarse grained beds from the lower part (73.90 m). Centre: Dark grey, finely laminated shale with macro fossils (67.75 m). Left: Highly bioturbated medium grey shale from the uppermost parts (59.66 m) of the cored Hekkingen Formation section.

In between the conglomeratic beds thinner sandstone beds occur. These are generally well sorted and show a decrease in grain size upwards, forming an overall fining-up succession. The sandstones show parallel lamination and rare cross-bedding, typical for tractional sediment transport. These conglomerates and sandstone beds are variously interpreted as turbidite and debris flow beds based on grain size and sorting as well as on clast- and matrix-support (Fig. 8). Such density flows may have formed along the central peak and the crater rim, representing the major modification phase of the crater (Dypvik et al. 2004b). Total organic carbon (TOC) content and Rock-Eval hydrogen index values (HI) (Espitalié et al. 1977) of the rocks from subunits IIb and IIc are variable, but much lower than in the overlying Hekkingen Formation (see below) shales (TOC: 0.6 - 4.5 wt%, average 1.6 wt%; HI: 51 - 328 mg/g TOC, average 130 mg/g TOC). Tmax values vary from 422-439°C and are on average about 10°C higher than in the Hekkingen Formation samples (432°C vs. 422 °C). This suggests that the Hekkingen Formation contributed little sediment to the Ragnarok Formation. This assumption is also supported by the sparse recovery of dinoflagellate cysts from the pre-impact Hekkingen Formation in this unit (i.e. only at 89.11m, 88.20 m and 97.93 m).

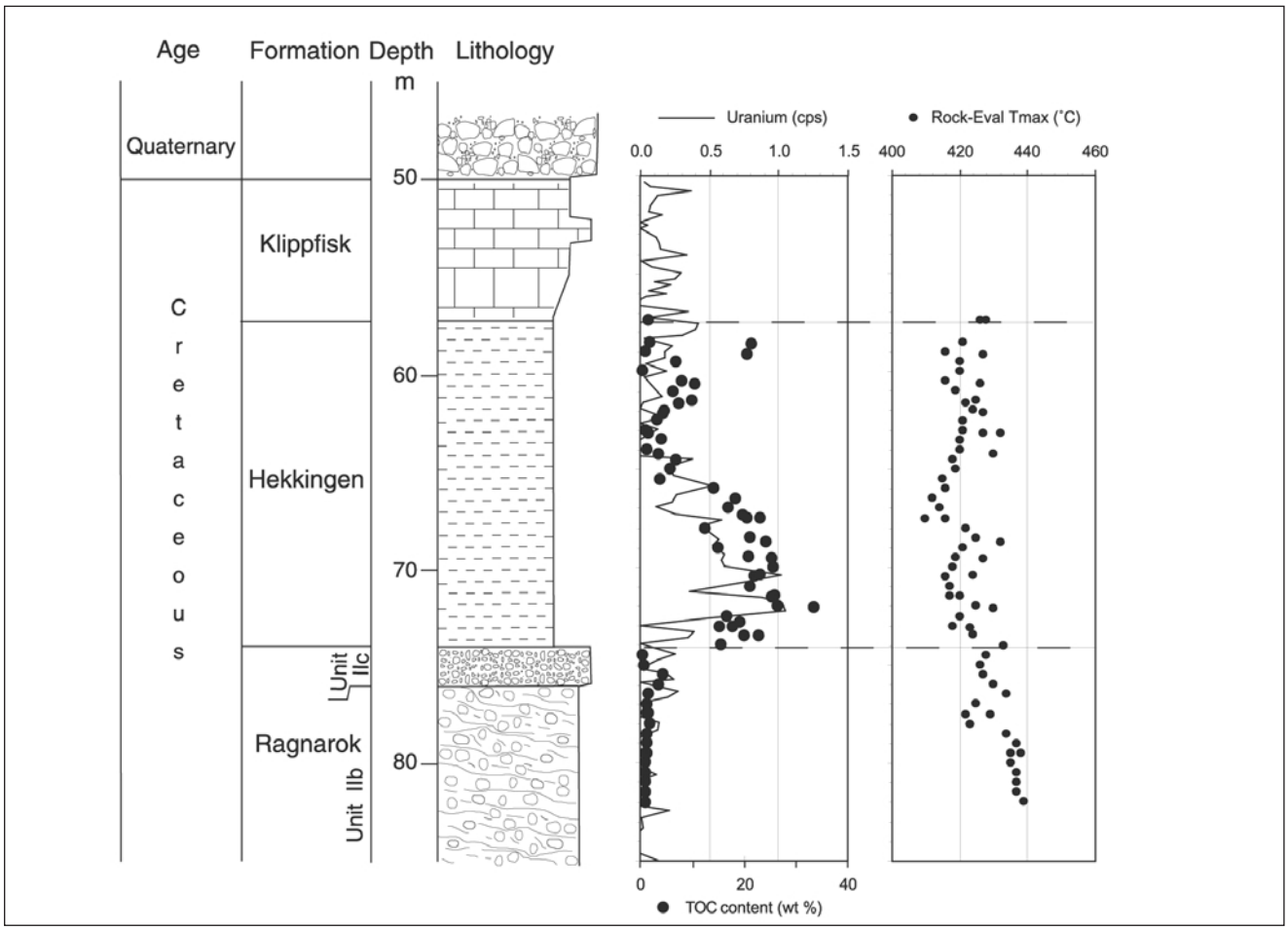

Fig. 10. Natural gamma radiation (uranium, measured on cores), total organic carbon content and Rock-Eval Tmax versus depth. Results from two sample series, collected at different times and analysed by different instruments, are plotted.

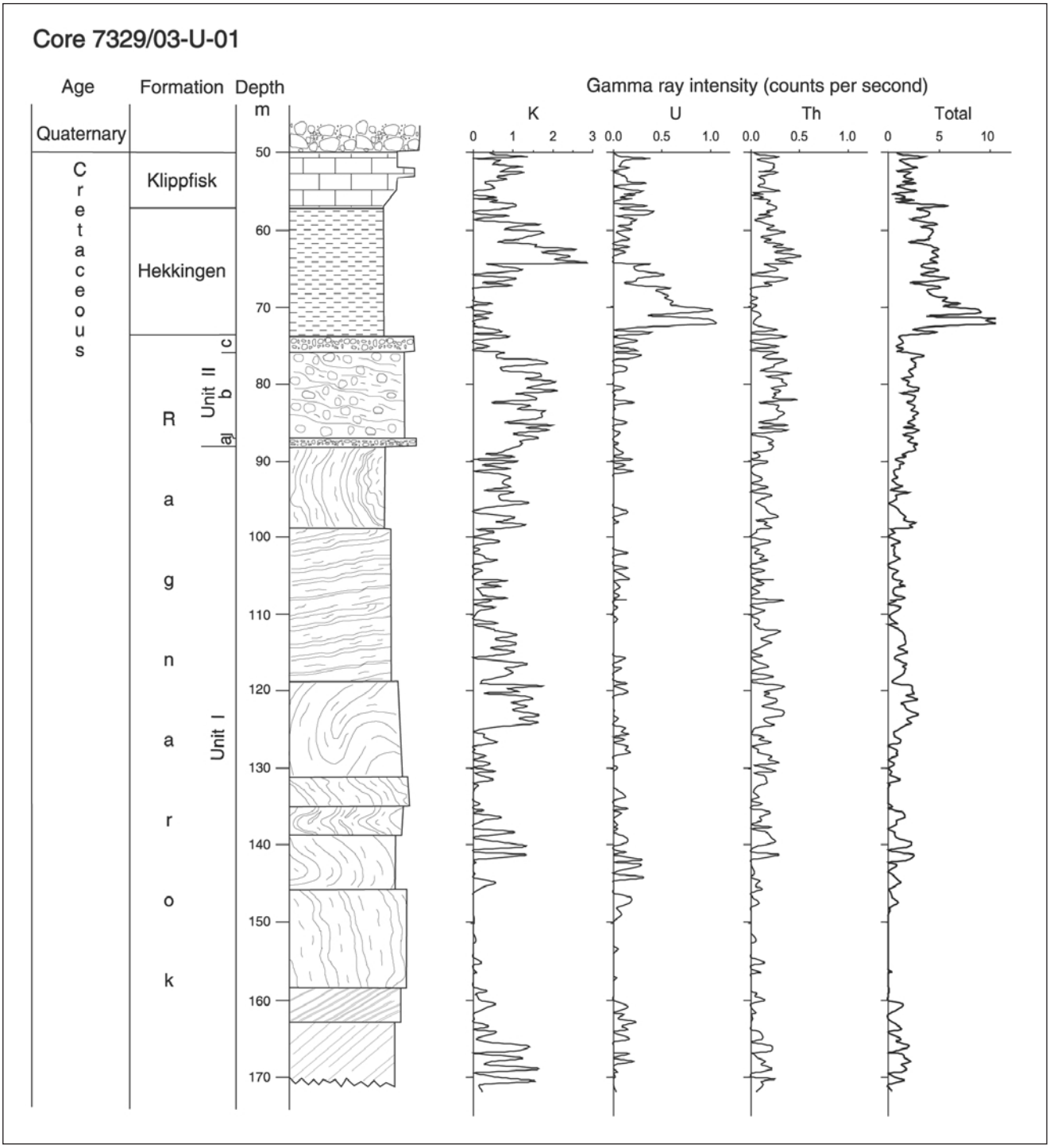

Fig. 11. Natural gamma radiation versus depth, measured on cores in the laboratory. The values are corrected for background radiation and the effects of overlapping radiation energy windows. Occasional negative values caused by overcompensation due to temporal variations of the background radiation during the measurement periods were set to zero.

Hekkingen Formation

The Hekkingen Formation in this core is represented by black to medium grey, organic-rich and laminated shales (74.05 - 57.20 m; Figs. 3 - 5, 8 - 9). The bivalve *Buchia* sp. is abundant throughout the formation, and some individuals have even preserved their nacreous aragonite inner coatings. The rocks contain abundant pyrite concretions (0.2 - 2 cm) and occasionally pinkish brown siderite concretions. The lithology is similar to that of the upper part of the same formation in the neighbouring core 7430/10-U-01 and elsewhere in the Barents Sea (Worsley et al. 1988; Leith et al. 1992) (Figs. 5 and 9).

The interval from 73.89 m to 73.78 m contains six very thin (5 cm to less than 1 cm thick) conglomeratic layers

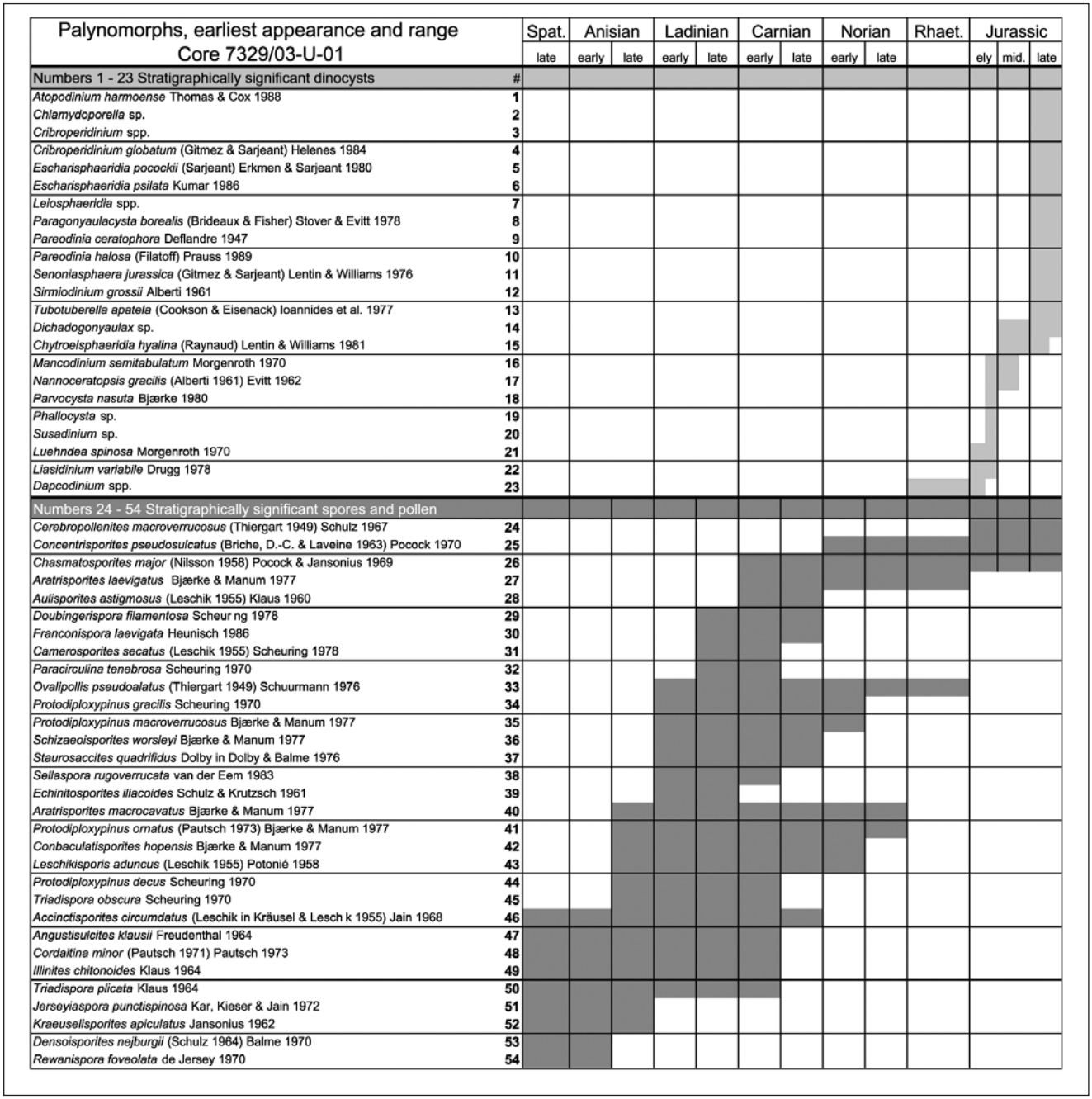

Fig. 12. Age-indicative palynomorphs of the Ragnarok Formation. Fig. 12a shows selected taxa sorted according to their earliest appearances. The total range of the individual taxa are marked by shading

(Figs. 5, 8 - 9). These are clast-supported and typically have a sharp, erosional base. The conglomerates contain dark grey clasts reworked from Hekkingen Formation shales, and clasts of a lighter grey colour, which have a composition similar to those in the conglomerates of unit IIc of the Ragnarok Formation.

The interval between 73.78 m and the top of the Hekkingen Formation (57.20 m) is dominated by parallel laminated shales, dark grey up to about 68 m depth and lighter grey in the remaining upper part of the interval (68 - 57.20 m) (Figs. 5, 8 - 9). Thin sections contain remnants of Prasinophytae algae (*Leiosphaeridia*) (20-50 μm in diameter) and enrichments in *Buchia* shell fragments. Between 65 m and 63 m no macrofossils were found, but they are again present in the upper part of the Hekkingen Formation from 63 to 57.10 m. Trace fossils (dominantly *Chondrites* and *Planolites*) and carbonate concretions are common at different levels in the upper part of the interval. Based on the macrofossils the post-impact Hekkingen Formation is dated as latest Volgian to earliest Ryazanian (Smelror et al. 2001).

Core data		Palynomorphs with stratigraphically restricted ranges		Dominant assemblage components
Depth *	Lithology **	Numbered as in Age indication Figure ***	Age span ****	Arranged according to frequency
77.80		54,**51**,**49**,48,47,44,41,40,**39**,**38**,36,35,28,27	Spathian - Norian	*Botryococcus,* indeterminate plankton, *Micrhystridium*
86.60	mudstone	49,44,42,41,**39**,**29**,**23**,**15**,**14**	Anisian - Late Jurassic	Indeterminate plankton, bisaccates, alete pollen
88.20	mudstone	49,47,45,44,43,41,13,12,11,10,9,8,7,6,5,4,3,2,1	Spathian - Late Jurassic	Indeterminate plankton, *Botryococcus,* bisaccates
89.11		54,49,48,46,45,42,**38**,36,**25**	Spathian - M. Jurassic	Bisaccates, striated pollen, smooth spores
93.07		54,53,**51**,49,48,47,43,41,**38**,37,36,**29**	Spathian - Carnian	Bisaccates, *Aratrisporites,* striated pollen
94.57A	shale gr-gy	**51**,49,47,46,45,44,43,42,41,37,33,32,31,27	Spathian - Rhaetian	Bisaccates, *Aratrisporites,* smooth spores
94.57B	shale gy	49,47,45,44,43,41,37,33,32,31,27	Spathian - Rhaetian	Bisaccates, *Aratrisporites,* smooth spores
97.81		**51**,**49**,48,47,46,45,43,42,41,**39**,37,36,33,**25**	Spathian - E. Jurassic	Bisaccates, smooth spores, perinate pollen
101.99	vf sst	49,47,45,43,42,40,33,30,28,27,**25**	Spathian - E. Jurassic	*Aratrisporites,* bisaccates, striated pollen
102.04	shale gy-gr	**51**,49,47,45,43,42,41,40,34,33,28	Spathian - Rhaetian	Bisaccates, *Aratrisporites,* striated pollen
104.50	vf sst gy	47,43,50,33,27,**25**,**19**	Spathian - E. Jurassic	*Aratrisporites,* bisaccates, smooth spores
107.58		47,45,42,41,40,**29**,**25**	Spathian - E. Jurassic	Bisaccates, striated pollen, *Aratrisporites*
112.20.A	shale gr-gy	**51**,47,43,40,33,30,28,**19**	Spathian - E. Jurassic	Bisaccates, smooth spores, *Aratrisporites*
112.20B	sst in shale	52,**51**,45,43,40,37,33,28,**19**,**18**	Spathian - E. Jurassic	Bisaccates, *Aratrisporites,* smooth spores
114.94	vf sst silty clay	**51**,48,43,40,28,**17**	Spathian - E. Jurassic	Bisaccates, *Aratrisporites,* smooth spores
115.09		47,45,40,33,**29**	Spathian - Rhaetian	Bisaccates, *Aratrisporites,* striated pollen
124.74	sst vf-f gy	47,43,40,33	Spathian - Rhaetian	Bisaccates, *Aratrisporites,* smooth spores
127.08		54,53,**51**,47,45,43,42,40,33	Spathian - Rhaetian	Bisaccates, *Aratrisporites,* ornamented spores
128.10A	shale gy-gr	50,49,48,44,43,40,35,33,26	Spathian - E. Jurassic	Bisaccates, *Aratrisporites,* striated pollen
128.10B	sst silt vf-f clasts	49,43,42,40,33,26,**25**	Anisian - M. Jurassic	Bisaccates, *Aratrisporites,* smooth spores
128.11		**51**,49,48,47,46,45,43,40,37	Spathian - Carnian	Bisaccates, striated pollen, *Aratrisporites*
135.91	mudst gy sst vf-f	49,47,43,40,33,**25**	Anisian - M. Jurassic	*Aratrisporites,* bisaccates, perinate pollen
141.36		**51**,**49**,47,46,45,43,42,40,30	Spathian - Carnian	Bisaccates, *Aratrisporites,* striated pollen
147.17	shale vf sst l	49,48,44,43,41,40,35,33,26,**25**,**24**,**18**	Spathian - E. Jurassic	*Aratrisporites,* bisaccates, smooth spores
153.77	sst vf-f gy	50,47,46,49,44,43,40,33,**25**,**23**,**21**,**18**	Anisian - E. Jurassic	Bisaccates, *Aratrisporites,* perinate pollen
156.20		54,53,**51**,48,43,41,27	Spathian - Norian	*Botryococcuss, Aratrisporites,* bisaccates
157.21		54,53,47,46,45,43,42,**29**,**25**	Spathian - M. Jurassic	Bisaccates, *Aratrisporites,* smooth spores
161.26		**51**,49,46,43,42,40,**25**	Spathian - M. Jurassic	Bisaccates, *Aratrisporites,* smooth spores
164.01		54,54,**51**,49,48,47,46,45,43,42,40,**38**,**29**,**25**	Spathian - M. Jurassic	Bisaccates, *Aratrisporites,* smooth spores
164.34		54,53,**51**,49,48,47,46,45,43,42,41,40	Spathian - Norian	Bisaccates, *Aratrisporites, Micrhystridium*
168.33		**51**,49,48,47,46,45,43,41,40,**29**	Spathian - Norian	Bisaccates, *Aratrisporites,* smooth spores
170.94A	shale gr	49,48,45,44,43,42,40,33,27,**25**,**17**	Spathian - M. Jurassic	Bisaccates, *Aratrisporites, Mircrhystridium*
170.94B	shale gr silt l	**51**,49,46,40,33,27,**25**,?**22**,**21**,**20**,**18**,**16**	Spathian - M. Jurassic	Bisaccates, *Aratrisporites, Mircrhystridium*

* Samples with low palynological productivity have been omitted
** Lithology of clasts described for the last batch of samples only
*** Bold types indicate taxa with short stratigraphic range
**** Age span includes all associations recorded

Fig. 12b displays the same information, presented according to sample depth. Note that most samples contain palynomorphs with quite different time ranges.

The organic matter is thermally immature, as seen in Rock-Eval, Tmax values of typically 420-432°C (Fig. 10) and production index (S1/(S1+S2)) values typically less than 0.05. The uranium curve derived from spectral gamma ray measurements shows a maximum at 67- 74 m depth and correlates with the organic richness (Figs. 10 and 11). The total organic carbon (TOC) content in the lower, laminated part of the Hekkingen Formation varies between 17 and 34%, which is similar to, and partly exceeds, the organic richness reported for this formation elsewhere in the northeastern Barents Sea (e.g. Bugge et al. 2002). High TOC values and hydrogen index values of 351 - 715 mg/g TOC indicate that the kerogen belongs mostly to type II and locally to type I, in a possible anoxic environment of deposition. Spectral gamma values for uranium in the upper part of the section (~68 - 57.10 m) are rather low. Organic richness and the hydrogen index of these rocks are more variable and generally lower than in the underlying interval (1.1 - 21.6 wt% TOC, HI = 49 - 574 mg/g TOC). This is consistent with the less oxygen-deficient depositional environment suggested by the variable, generally lighter colours and the occasional bioturbation of these deep shelf deposits.

Klippfisk Formation

The 7.1 m thick interval representing the Klippfisk Formation consists of heavily bioturbated, light greenish-grey, argillaceous carbonates (marls) (Figs. 3 - 5). The lithology is similar to that of the Klippfisk Formation in the type well 7430/10-U-01, described by Smelror et al. (1998) as representing a condensed carbonate platform. The top of the formation is not preserved at this locality as the overlying till rests directly on the marls of the Klippfisk Formation.

Spectral gamma results

Natural spectral gamma radiation (K, U, Th, total) was measured on the core in the laboratory (Fig. 11). The total and spectral readings for the Klippfisk and Hekkingen formations in core 7329/03-U-01 are similar to those found in the neighbouring core 7430/10-U-01. The total gamma activities in the cored Ragnarok Formation are significantly lower than those of the Hekkingen Formation, and the spectral intensities for uranium are close to the detection limit (Figs. 10

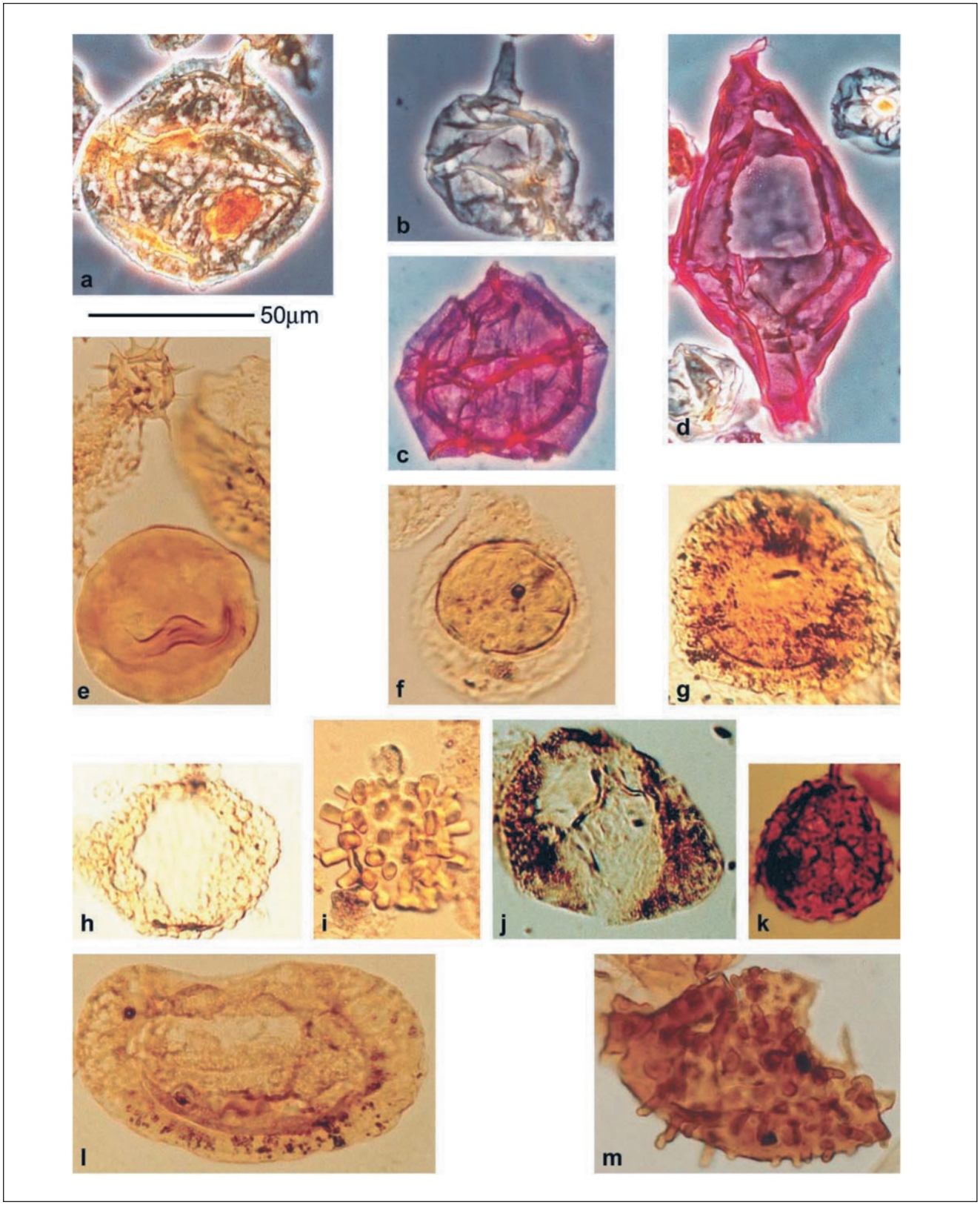

Fig. 13. Palynomorphs from the Ragnarok Formation. The 50 µm scale indicates the enlargement of the palynomorphs. The number following each name refers to Fig. 12 where occurrences are plotted. ***a)*** *Cribroperidinium globatum (Gitmez & Sarjeant) Helenes 1984, #4, sample 88.20 m.* ***b)*** *Pareodinia ceratophora Deflandre 1947, #9, sample 88.20 m.* ***c)*** *Sirmiodinium grossii Alberti 1961, #12, sample 88.20 m.* ***d)*** *Tubotuberella apatela (Cookson & Eisenack) Ioannides et al. 1977, #13, sample 88.20 m.* ***e)*** *Tasmanites sp. and Micrhystridium sp. (the upper left corner) sample 164.34 m.* ***f)*** *Aulisporites astigmosus (Leschik) Klaus 1960, #28, sample 77.8 m.* ***g)*** *Doubingerispora filamentosa sample Scheuring 1978, #29, 77.80 m.* ***h)*** *Protodiploxypinus macroverrucosus Bjærke & Manum 1977, #35, sample 77.80 m.* ***i)*** *Echinitosporites iliacoides Schulz & Krutzsch 1961, #39, sample 77.80 m.* ***j)*** *Triadispora obscura Scheuring 1970, #45, sample 93.7 m.* ***k)*** *Rewanispora foveolata de Jersey 1970, #54, sample 164.34.* ***l)*** *Illinites chitonoides Klaus 1964, #49, sample 164.34 m.* ***m)*** *Jerseyiaspora punctispinosa sample Kar, Kieser & Jain 1972, #51, 164.34 m.*

and 11). Uranium is known to be associated with organic material, and gamma readings in homogeneous lithologies therefore commonly correlate with organic matter content (e.g. Supernaw et al. 1978; Schmoker 1981; Fertl & Rieke 1980; Dypvik & Eriksen 1983). The low uranium gamma values in the Ragnarok Formation suggest that the Hekkingen Formation, which was still unconsolidated when the impact occurred, contributed little sediment to the Ragnarok Formation, in agreement with the palynological observations (see below).

The pronounced increase in K-activity at 65 m in the Hekkingen Formation may reflect a decrease in smectitic fractions and an increase in illitic components (Fig. 11). This is hinted at by Dypvik et al. (2003), who demonstrated an increase in the illitic components towards the one sample (60.00 m) analysed from the Hekkingen Formation interval shallower than 65 m.

Palaeontological characteristics

The marine macro- and microfaunas of core 7329/03-U-01 have previously been described by Smelror et al. (2001) and Bremer et al. (2003). The very prolific bloom of the prasinophycean alga *Leiosphaeridia* in the oldest post-impact sediments of the Hekkingen Formation has been documented in detail by Smelror et al. (2002).

Below we give an overview of the palyno-floras found in the Ragnarok Formation. The main purpose of these analyses has been to document the ages of the rocks from which the impact breccia is derived. Altogether 117 palynomorph taxa have been recognised in core 7329/03-U-01. Palynomorphs derived from terrestrial sources dominate and indicate that the formation comprises rocks of different ages. Figures 12 and 13 present the stratigraphic ranges of 39 stratigraphically important taxa.
Only age-significant taxa are commented in the following:

- *Illinites chitonoides* and *Jerseyiaspora punctispinosa* occur regularly and range from the Upper Spathian to the Carnian. *J. punctispinosa* is restricted upwards to middle Anisian deposits. Both *Densoisporites nejburgii* and *Rewanispora foveolata* have ranges restricted upwards to the Lower Anisian deposits (Figs. 12 and 13).
- *Aratrisporites macrocavatus* and *Conbaculatisporites hopensis* among others characterize the Upper Anisian to Ladinian of the Sassendalen Group on the Svalis Dome. On Svalbard these taxa continue into the Carnian of the Kapp Toscana Group (J.O.Vigran, unpublished data). Bjærke & Manum (1977) reported them from Hopen and Kong Karls Land (Kapp Toscana Group; De Geerdalen and Wilhelmøya formations).
- *Echinitosporites iliacoides* is restricted to the Ladinian on Svalbard and the Barents Sea Shelf (Vigran et al. 1998). *Ovalipollis pseudoalatus, Schizaeoisporites worsleyi* and *Sellaspora rugoverrucata* have been recorded from the Lower Ladinian on Svalbard and the Barents Sea Shelf, Svalis Dome (Vigran et al. 1998).
- An Upper Ladinian - Lower Carnian association is recognized on the basis of *Aulisporites astigmosus, Camerosporites secatus, Chasmatosporites major, Doubingerispora filamentosa* and *Paracirculina tenebrosa*. It should, however, be noted that most of the evidence described by from the Upper Triassic deposits of Hopen and Kong Karls Land has not been recorded in this core.
- *Cerebropollenites macroverrucosus* has the lowest appearance in rocks of early Early Jurassic age. Poorly preserved specimens recorded as Early Jurassic dinocysts (Fig. 12, Nos 16-23) confirm that Lower Jurassic deposits are represented throughout the Ragnarok Formation.

The palynomorph content suggests that the slumped sediments forming the Ragnarok Formation in core 7329/03-U-01, interval 170.94 - 89.11 m (most of unit I) has its major source Middle Triassic deposits of the Sassendalen Group. Some of the palynomorphs probably represent the Lower Carnian, i.e. the oldest deposits of the Wilhelmøya Subgroup, but there is no palynological evidence indicating a Carnian-Norian association from the Kapp Toscana Group. Evidence of Lower Jurassic rocks generally occurs in minor proportions.

Samples in the 88.20-77.80 m interval, representing the uppermost part of the Ragnarok Formation (uppermost part of unit I, subunits IIa and most of subunit IIb), contain a stratigraphic mixture of pollen and spores from the Middle to Upper Triassic and Lower Jurassic. The dominance of *Botryococcus* and marine plankton of presumed Jurassic age distinguishes these samples from those in the lower part of the core that contain dominantly terrestrial material.

One sample at 86.20 m contains dinoflagellate cysts of late Middle to early Late Jurassic affinity (i.e. *Dichadogonyaulax* sp. and *Chytroeisphaeridia hyalina*). Three samples from 89.11 m , 88.20 m and 87.93 m include Late Jurassic dinoflagellate cysts in addition to the Late Triassic to Early Jurassic terrestrial palynomorphs. Characteristic species found in these samples are *Atopodinium haromense, Paragonyaulacysta borealis, Cribroperidinium* spp. (including *C. globatum*), *Senoniasphaera jurassica* and *Tubotuberella apatela*. They are derived from the pre-impact deposits of the Hekkingen Formation.

Impact-induced disturbance

Seismic reflectivity patterns

Seismic reflection profiles at Mjølnir (Figs. 2 and 14) confirm the presence of a 850 - 1400 km^3 volume of

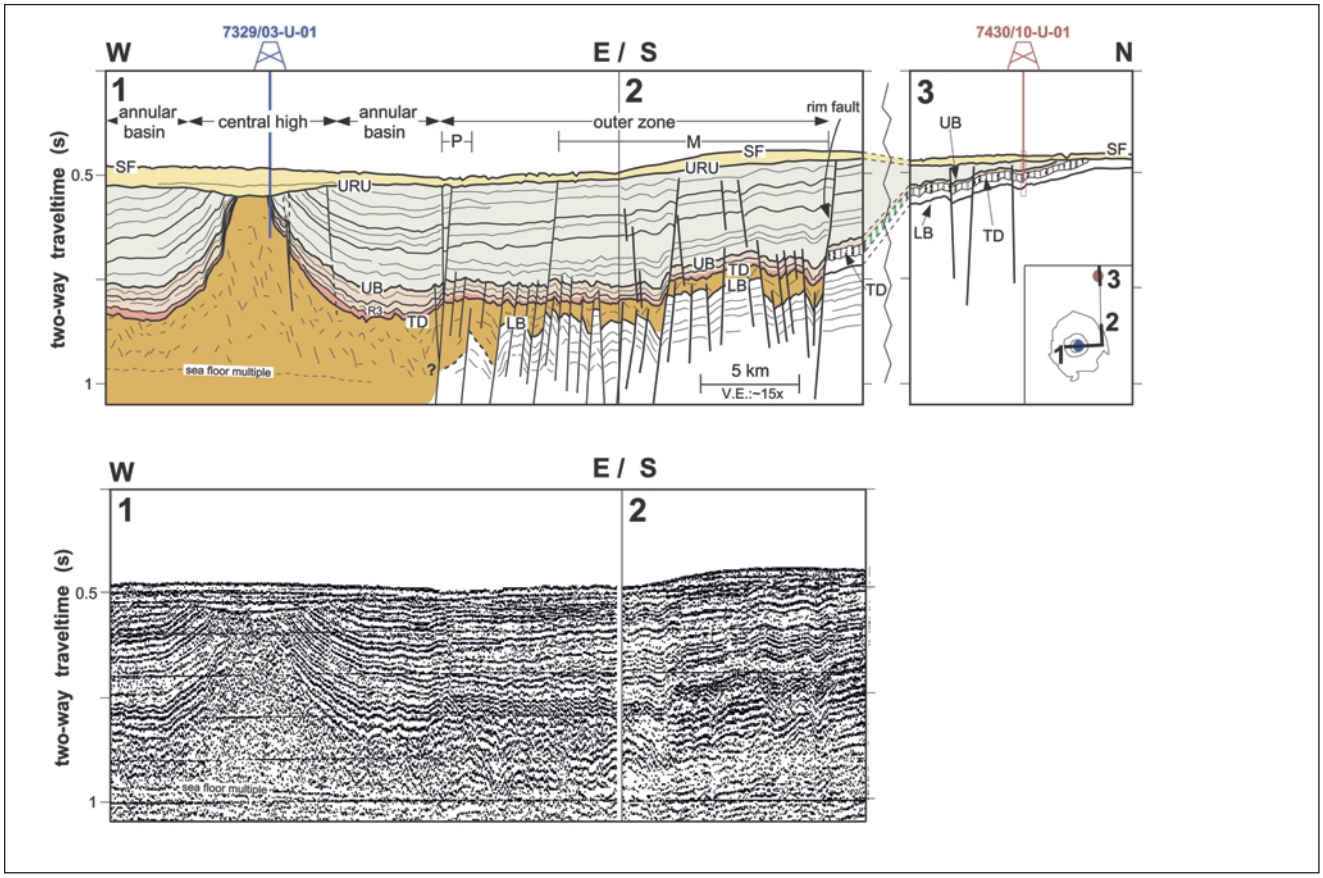

Fig. 14. Interpreted (top) and uninterpreted (bottom) examples of shallow multi-channel profiles crossing the Mjølnir structure and providing the seismic correlation between the two shallow boreholes. Reflectors UB and LB constrain the time of impact. SF, sea floor; URU; late Cenozoic upper regional unconformity; UB, lower Barremian; TD (impact horizon), the first continuous reflector above the seismic disturbance; R3, top of gravity flows imposed by the Mjølnir impact (cf. Fig. 4); LB, base Upper Jurassic. Vertical bars (raster) denote the uncertainty in the seismic tie of the impact horizon. P, peak ring; M, marginal fault zone (from Tsikalas & Faleide 2003).

sediments characterized by disturbed seismic reflectivity patterns. The pervasive disturbance is sharply bounded above by reflector TD (top disturbance), which corresponds to the crater surface immediately after the impact (Figs. 2a-b, 3 and 14). There is a systematic loss of reflection coherency in the deeper and outer parts of the disturbance, up to its upper and central parts caused by a progression of seismic characteristics from disrupted layering and diffractions to chaotic and reflection-free zones. Tsikalas et al. (1998a) subdivided the seismic disturbance into an intensely disturbed zone and a less disturbed transitional zone (Fig. 2a). The main criterion used to delimit the intensely disturbed zone is the complete loss of correlatable platform stratification. This largely corresponds to the location where downward bending Triassic strata encounter steeply upward bending strata, beneath the annular basin and the central high. Within the intensely disturbed zone considerable transport of material appears to have taken place. The zone contains only a few reflector segments that remain subhorizontal and enclose the reflection-free seismic facies, which is probably related to the destruction of large-scale coherent features by the cratering process. In contrast to the intensely disturbed zone, elements of correlatable platform stratification can be recognized within the transitional zone. The intensely disturbed zone fades out just above the regionally prominent Top Permian reflector, while the surrounding transitional zone extends below the reflector (Fig. 2a).

Excavated crater and structurally uplift outcome: the Ragnarok Formation

In the shallow periphery of the structure, prominent fault blocks are present (Fig. 14) and the observed disturbance is floored by uniformly layered strata which can be traced into the surrounding undisturbed platform (Figure 2a). Farther inward, clear definition of the fault-blocks is lost and the unit becomes progressively dominated by disrupted and chaotic reflections, diffractions, and reflection-free zones (Figs. 2 and 14). This makes it difficult, in most cases, to identify exactly the boundary between the two units as the central part of the disturbance is approached. However, on some profiles the boundary is marked by a characteristic, near-continuous, low-frequency reflector (Fig.15). The upper unit corresponds to the Ragnarok Formation

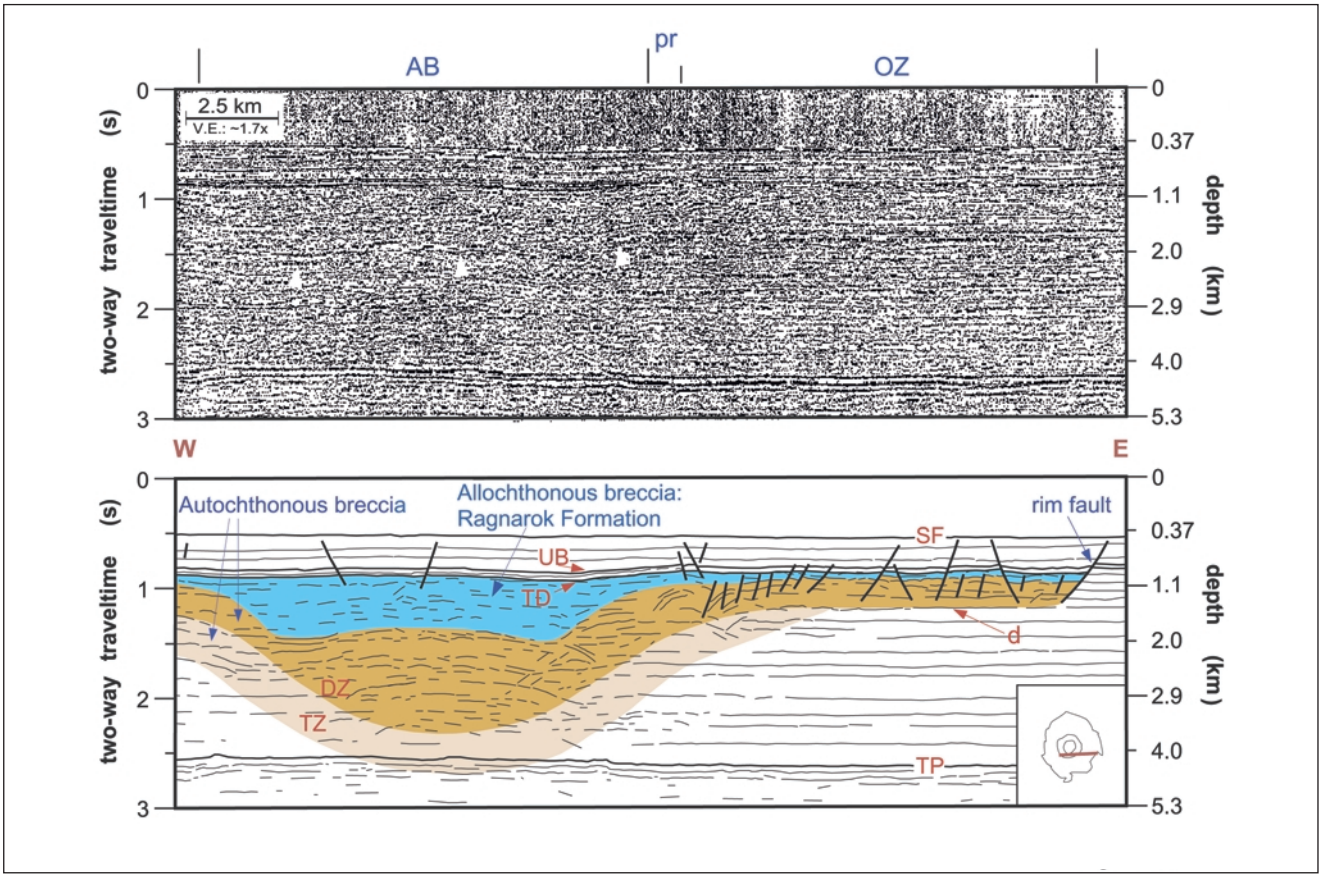

Fig. 15. Conventional multi-channel seismic profile, and interpretation, across the crater rim. The allochthonous breccia corresponds to the Ragnarok Formation, while the autochthonous breccia corresponds to the area of intense disturbance, DZ, and the transitional area of less disturbance, TZ. White arrows show the position of the near-continuous, low-frequency reflector beneath the annular basin (AB); d, low-angle décollement. Other annotations are as in Fig. 14 (from Tsikalas et al. 1998a).

containing allochthonous and parautochthonous breccia, expected to consist of crushed fall-back and backwash material containing melted rock; and structurally uplifted, slumped and inverted targeted material from deeper levels. Similarly, the lower unit probably corresponds to the extensively in-situ fractured and mixed autochthonous breccia (Fig. 15) (Tsikalas et al. 1998a). Based on detailed observations on seismic reflection profiles the structural uplift beneath the central high was estimated to be 1.5 to 2 km (Tsikalas et al. 1998a), while the theoretically predicted value (e.g. Cintala & Grieve, 1994) based on Mjølnir dimensions is as much as 2.5-3km. The cross-sectional shape of the Ragnarok Formation can be described as consisting of two elements (Figs. 14 and 15): (1) a ~ 4 - 6.5 km wide annular trough beneath the present annular basin with fairly steep and well defined flanks and a maximum depth of ~1.0 - 1.3 km, and (2) a thinner unit that fills in the block-faulted relief beneath the outer zone, ranging in thickness from 0.05 to 0.2 km (Tsikalas et al. 1998a). On the basis of seismic observations and numerical simulations an estimated 180 - 230 km^3 excavated/ejected material volume was displaced from the impact-site and re-deposited in the near vicinity (Tsikalas et al. 1998a; Shuvalov et al. 2002; Shuvalov & Dypvik 2004).

The Ragnarok Formation is expected to contain a quantity amount of dispersed melts as the energy release during a large meteorite impact is sufficient to shock-heat target rock material to the point of melting (e.g. Melosh 1989). According to the empirical relationship of Cintala & Grieve (1994), an impact leading to a structure of Mjølnir's size is expected to have generated a melt volume of ~10 - 30 km^3. Because of the lack of identifiable melt-derived reflectors at Mjølnir, Tsikalas et al. (1998b) interpreted the low-amplitude magnetic anomalies over the structure in terms of dislocation of weakly magnetized platform strata, perhaps associated with local concentrations of melts or minor melt dykes in the peripheral region. Dypvik & Ferrell (1998) found smectite in core 7430/10-U-01 that may represent an alteration product from impact glass, the only possible indication of a melt found so far.

Extensive crater collapse and resurge gullies

Geophysical observations and numerical simulations constrain the transient cavity (referred to the impact

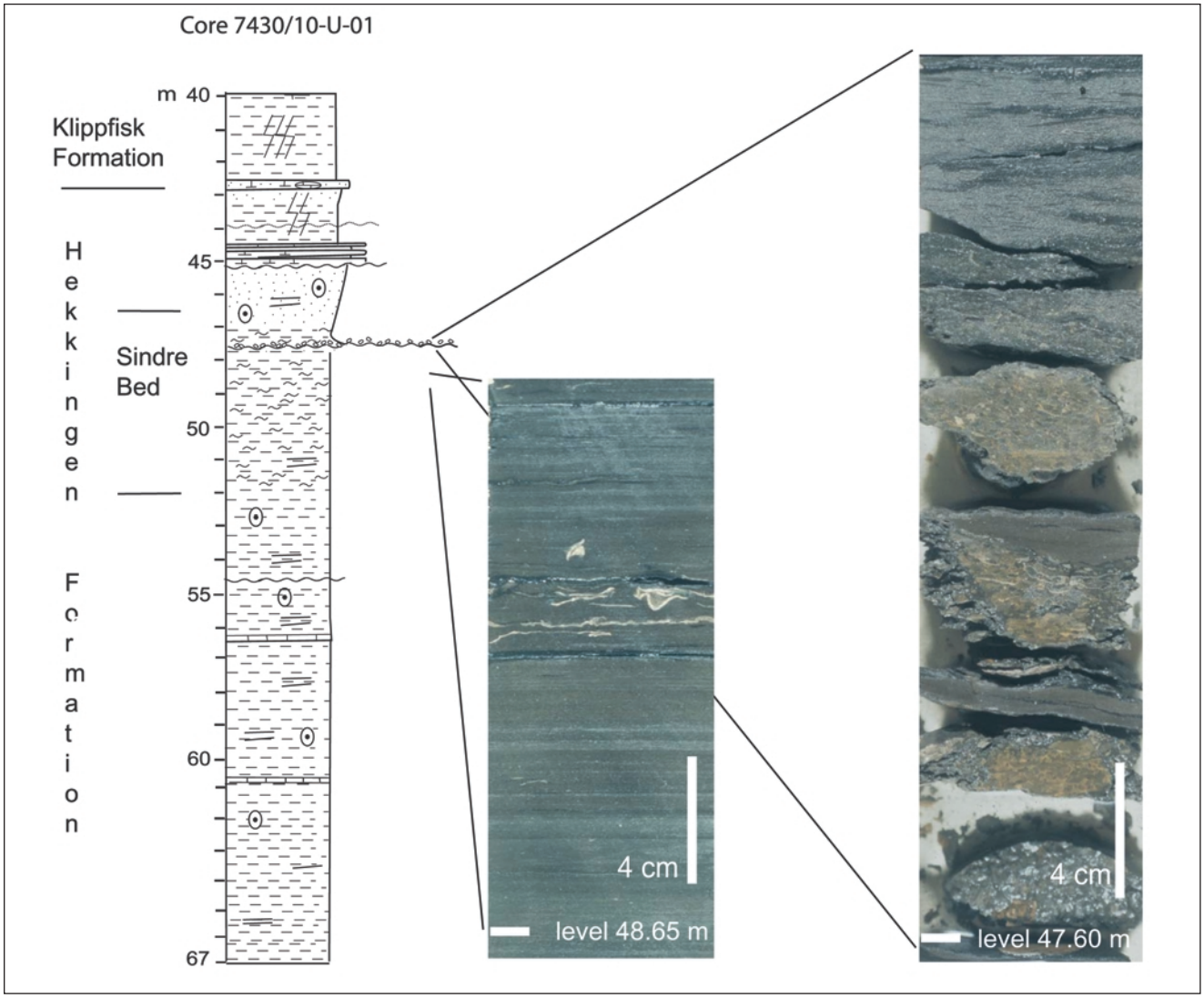

Fig. 16. Log of core 7430/10-U-01 showing the development of the Sindre Bed within the Hekkingen Formation. The core photo to the right shows the 19 cm thick, three turbidite beds containing grains of shocked quartz. The photo to the left shows the typical lithology of the Hekkingen Formation. The wave symbol (~) in the Sindre Bed illustrates presence of smectite.

cratering stage prior to crater collapse) to have had a diameter and depth of 16 - 20 km and 4.5 - 6 km, respectively (Tsikalas et al. 1998a; Shuvalov et al. 2002). The ratio of the final crater diameter to the transient cavity diameter is referred to as the collapse factor. The value of this parameter is normally considered to lie in the range of 1.4 - 2.0, with an average value of 1.6 (Melosh 1989). Assuming the average value of 1.6, an impact structure with a transient cavity diameter of 16 - 20 km would therefore be expected to have a final diameter of 26 - 32 km. By contrast, Mjølnir's 40 km final diameter corresponds to a collapse factor of 2.0 - 2.5. Hence, the Mjølnir crater expanded to a large degree during gravitational collapse, in accordance with other marine impacts (Dypvik & Jansa 2003).

The cratering processes triggered by the Mjølnir impact resulted in a shallow crater without a raised crater rim (Figs. 2, 14 and 15). Geophysical observations and numerical simulations (Tsikalas et al. 1998a-c; Shuvalov et al. 2002) clearly show that these features can be related to the large degree of collapse, and extensive infilling coeval with the collapse caused by the low-strength siliciclastic sedimentary target within the upper 3 km. Outward widening of the structure resulted from the inward collapse of the initial crater rim on faults floored by apparent low-angle décollement surfaces. The impact of the Mjølnir projectile in the Barents Sea gave rise to a water cavity also. Collapse of the water cavity caused a turbulent resurge of water and material flowed back to the crater site through a system of erosional/depositional resurge gullies, accounting for both the extensive infilling and the lack of a raised crater rim (Tsikalas & Faleide 2003). Three prominent resurge gullies are identified at Mjølnir located within a 10-15 km radius outside the crater rim wall. These vary in depth from 30 - 70 m, in width from 1 - 5 km, and in length from 5-25 km (Tsikalas & Faleide 2003). The

gullies exhibit meandering and bifurcating patterns and cut the rim faults where they have channelized resurge sediments from the surrounding platform. These are mixed with near-field excavated/ejected target material and the denser/heavier portions of the fall-back ejecta, providing an extra resurge infilling volume at Mjølnir in the order of 50 km^3 (Tsikalas & Faleide 2003).

Ejecta outside the Mjølnir crater – core 7430/10-U-01: The Sindre Bed

Outside the Mjølnir crater rim the deposits of the Ragnarok Formation thins dramatically and are mainly represented by airborne or reworked ejecta. These beds consist of highly varied lithologies, with large lateral variations, since they reflect the combination of general local sedimentation and the exotic Mjølnir ejecta. Ejected deposits may be found thousands of kilometres from impact sites (Melosh 1989; French 1998).

The ejecta from the Mjølnir impact are found as separate beds within the Hekkingen Formation or time-equivalent units in more distal areas (Dypvik et al. 2004b). We suggest naming the ejecta bed outside the Mjølnir crater the Sindre Bed. Sindre is the name of the dwarf and blacksmith who made Tor's hammer Mjølnir. Forging the hammer involved lots of sparks, fire and glowing melts, which is also the meaning of the name Sindre (cinder, hammer-scale), a suitable name for air borne ejecta from the Mjølnir crater. In the lower shaly part of the Sindre Bed in core 7430/10-U-01, Dypvik & Ferrell (1998) found large amounts of smectite, which they interpreted to represent altered impact glass.

Borehole 7430/10-U-01 was drilled 30 km NNE of the rim of the Mjølnir crater (Table 1 and Figs. 1 and 16). From the core-base (67.6 m) to the base of the Sindre Bed (52.0 m) the core consists of finely laminated, dark grey, organic-rich shales typical of the Hekkingen Formation in the Barents Sea area. From 52 m to 46.5 m the core contains sediments defined to belong to the Sindre Bed (Fig. 16). The interval from 52 m to 47.60 m consists of dark grey, smectitic claystones and shales, with dispersed mudflake clasts. This unit is directly overlain by the organic-rich, finely laminated, dark grey claystones of the Hekkingen Formation (Dypvik et al. 1996; Dypvik & Ferrell 1998). At 47.60 - 47.40 m three much coarser, sand- to gravel-sized, upwards fining conglomeratic units are found separated by mm to cm thick claystone/shale laminae. This 19 cm thick package is succeeded by 120 cm of sandy and silty shales (47.40 - 45.20 m), which have a well-defined iridium peak at 46.85 m (Dypvik & Attrep 1999). The very last geochemical ejecta-signal is found at 46.5 m, and is consequently used to define the top of the Sindre Bed. The uppermost boundary of the cemented siltstones of Hekkingen Formation in this core (45.20 m) is represented by an erosional boundary towards the overlying bioturbated, marly claystones of the Klippfisk Formation (45.2 m). It is difficult in this case to evaluate how much material has been removed. This uppermost part of the Hekkingen Formation (46.5 - 45.2 m) is heavily bioturbated and contains fossil fragments.

The Sindre Bed has been recognised in its type section in core 7430/10-U- 01, on Svalbard and in other cores from the Barents Sea (Dypvik et al. 2004b). A feature that can be correlated over very long distances is the extreme Ir-enrichments published from time-equivalent beds in Nordvik, Siberia, about 2500 km to the northeast (Zakharov et al. 1993). Applying the estimate of an impact from the southwest at an angle of about 45 degrees (Tsikalas 2004), along with the ejecta distribution simulations of Shuvalov & Dypvik (2004), the most probable area to track the thicker developments of the Sindre Bed will be northeast of the Mjølnir crater, towards Siberia, e.g. Nordvik (Shuvalov & Dypvik 2004). The thickness distribution modelled is uneven. The areal distributions of the Mjølnir ejecta and the Sindre Bed are, however, even more complex due to the effects of the immediate post-impact tsunami and ocean currents.

Conclusions

The Ragnarok Formation encompasses the allochthonous, brecciated sediments that originate from the excavation and modification of the Mjølnir impact crater in the Barents Sea. The formation includes deposits of avalanches, slides, mass flows and density currents along with large slumped units of beds that were partly deformed while still soft (units I, IIa,IIb,IIc). The chaotic depositional patterns of the formation are also in accordance with the complex and out-of-order biostratigraphy of the folded, fractured and deformed beds. Accordingly, the geophysical characterisation of the Ragnarok Formation shows chaotic reflections, indicating a formation thickness up to more than one kilometre. The definition of the Ragnarok Formation within the deposits of the Mjølnir crater is based on studies of the 121 m long Mjølnir core (7329/10-U-01) along with geophysical interpretations of mainly high-resolution seismic lines. The lack of available core material from outside the crater rim explains why the Ragnarok Formation in those areas, so far, can only be described as a sedimentary wedge on the seismic lines. In addition to the Ragnarok Formation, the Sindre Bed has been defined. This bed consists of ejected material from the Mjølnir crater. It has been identified in cores from the Barents Sea. Its correlative, long distance equivalents may be recognised in an onshore section in Svalbard and in central Siberia (Nordvik region).

Table 1. Technical data for coreholes 7329/03-U-01 and 7430/10-U-01: lithologies, boundaries and references. All depths in metres below seabed. The definitions of the Ragnarok Formation (core7329/03-U-01) and Sindre Bed (core 7430/10-U-01) are shown.

Unit	Thick-ness m	Top depth m	Base depth m	Lithology	Upper boundary	Lower boundary	Age	Reference	Comment
Quaternary	**50**	**0**	**50**	**Till**					**Soil drilling**
Klippfisk Fm.	**7.10**	**50.10**	**57.20**	**Greenish marls**	**A break towards Quaternary till**	**Green marls on dark grey Hekkingen shales**	**Late Berriasian - Hauterivian**	**Smelror et al., 1998**	**core drilling**
Hekkingen Fm.	**16.85**	**57.20**	**74.05**	**Dark grey shales**	**Green marls on dark grey Hekkingen shales**	**Dark grey shales on light grey Ragnarok conglomerates**	**Late Oxfordian – Early Berriasian**	**Worsley et al., 1988**	**core drilling**
Ragnarok Fm.	**96.95**	**74.05**	**171.00**	**Cgl., sst. and shales**	**Dark grey shales on light grey Ragnarok conglomerates**	**Not exposed**	**Latest Volgian or earliest Berriasian**	**New formation, this paper**	**core drilling**
Unit II	14.30	74.05	88.35	See table 2	See table 2	See table 2			core drilling
Subunit IIc	1.68	74.05	75.73	See table 2	See table 2	See table 2			core drilling
Subunit IIb	11.70	75.73	87.43	See table 2	See table 2	See table 2			core drilling
Subunit IIa	0.92	87.43	88.35	See table 2	See table 2	See table 2			core drilling
Unit I	82.65	88.35	171.00	See table 2	See table 2	See table 2			core drilling
Total well depth	171.00		171.00						
Total core length	121.00								
Produced display cuts	62.00								
Core 7430/10-U-01									
Sindre Bed	**3.50**	**46.50**	**52.00**	Grey, smectitc shales and conglomerates	The final Ir-enrichment defines the top of the Sindre Bed	Dark grey smectitic shales on dark grey, low –smectitic, laminated dark grey shales	Latest Volgian or earliest Berriasian	**New formation, this paper**	**Core drilling**

Table 2. The stratigraphical subdivision of core 7329/3-U-01

Stratigraphic unit	Depth	Lithology	Depositional conditions
Klippfisk Formation	50.00 – 57.20 m	Very light greenish grey marls and carbonates, fossiliferous.	Bioclastic carbonate sedimentation
Hekkingen Formation	57.20 – 68.00 m	Light grey shales laminated, in some parts no fossils. From 63 m and up core, rich in bioturbation.	Suspension deposition
	68.00 – 73.78 m	Dark grey to black organic-rich shales, rich in fossils. Parallel lamination.	Suspension deposition
	73.78 – 73.89 m	Interval with 6 thin clast zones, distal debris flows. Parallel laminated dark shales surrounding the clast rich beds	Debris flows
	73.89 – 74.05 m	Dark grey to black organic rich shales, rich in fossils. Parallel lamination.	Suspension deposition
Unit IIc Ragnarok Fm.	74.05 – 74.31 m	Matrix- and grain supported conglomerate, faintly laminated.	Debris flow
	74.31 – 74.37 m	Parallel laminated medium sandstones.	Turbidite flow
	74.37 – 74.71 m	Homogeneous, grain-supported with possible inverse grading.	Debris flow
	74.71 – 74.81 m	Medium-grained sandstone, planar cross bedding, well sorted.	Turbidite or current reworked
	74.81 – 75.27 m	Mainly clast supported conglomerate, general inverse grading with faint cross-bedding.	Debris flow
	75.27 – 75.33 m	Fining upwards clay clast conglomerate, matrix supported.	Turbidite
	75.33 – 75.42 m	Matrix supported conglomerate, clay clasts.	Mud flow? – turbidite?
	75.42 – 75.48 m	Matrix supported conglomerates with thin clay bed.	Mud flow? – tubidite?
	75.48 – 75.54 m	Clay with clay clasts, matrix supported.	Mud Flow? – turbidite?
	75.54 – 75.61 m	Thin clay bed overlain by a homogeneous, clast-supported conglomerate.	Debris flow
	75.61 – 75.73 m	Homogenous, clast-supported.	Debris flow
Unit IIb Ragnarok Fm.	75.73 – 79.50 m	Dark grey to brown, olive green, highly fragmented claystones, in parts clast-supported.	Autobrecciation, mud flow
	79.50 – 83.00 m	Homogeneous part with rather few clasts, faint lamination.	Sliding?
	83.00 – 87.43 m	Dark grey to brown, olive green, highly. fragmented claystones, partly clast-supported.	Autobrecciation, mud flow
Unit IIa Ragnarok Fm.	87.43 – 87.70 m	Matrix supported conglomerate, inverse grading.	Debris flow
	87.70 – 88.09 m	Matrix supported conglomerate, inverse grading.	Debris flow
	88.09 – 88.30 m	Matrix supported, homogenous conglomerate.	Debris flow
	88.30 – 88.35 m	Siderite bed, septarian lower part and laminated darker brown upper part.	
Unit I –Ragnarok Fm.	88.35 –171 m	Folded and fractured bedded sandstones, siltstones and shales with a few alternating carbonate beds. 120 cm brecciated interval on top.	Slumps and slides along the rising central high, collapsing crater

Acknowledgements: Norsk Hydro ASA, Phillips Petroleum Company Norway, Saga Petroleum ASA and Statoil ASA are thanked for financial support of the drilling operation. M/V 'Bucentaur' and the Norwegian Petroleum Directorate also supported the operation by making it possible for the Mjølnir group to borrow the boat this August for a week at very short notice and at a good rate. The drilling crew (Dia-Team) and the crew of the drillship 'Bucentaur' carried out excellent work. Thanks are due to Joar Sættem for great help during the drilling operation and to Øistein How for valuable laboratory assistance. We would also like to thank Erik Simensen for discussions on Nordic mythology. The Mjølnir project was financially supported by the Norwegian Research Council and benefited from close scientific cooperation with the ESF Impact program. The comments of K-S. Lervik, P.B. Wignall, S.P. Hesselbo and one anonymous referee are highly appreciated.

References

Bjærke, T.A. 1977: Mesozoic palynology of Svalbard II. Palynomorphs from the Mesozoic sequence of Kong Karls Land. *Norsk Polarinstitutt Årbok 1976, 83 -120.*

Bjærke,T.A. & Manum, S.B. 1977: Mesozoic palynology of Svalbard – I. The Rhaetian of Hopen, with preliminary report on the Rhaetian and Jurassic of Kong Karls Land. *Norsk Polarinstitutt Skrifter 165,* 1- 48.

Bremer, G.A.M, Smelror, M., Nagy, J. & Vigran, J.O. 2004: Biotic responses to the Mjølnir meteorite impact, Barents Sea: Evidence from a core drilled within the crater. *In* Dypvik, H., Burchell, M. & Claeys, P.(eds.): *Cratering in marine environments and on ice.* Springer Verlag, Heidelberg, 21-38.

Bugge, T., Elvebakk, G., Fanavoll, S., Mangerud, G., Smelror, M., Weiss, H.M., Gjelberg, J., Kristensen, S.E. & Nilsen, K. 2002: Shallow stratigraphic drilling applied in hydrocarbon exploration of the Nordkapp Basin, Barents Sea. *Marine and Petroleum Geology 19,* 13-37.

Cintala, M.J. & Grieve, R.A.F. 1994: The effects of differential scaling of impact melt and crater dimensions on lunar and terrestrial craters; some brief examples. *In* Dressler, B.O., Grieve, R.A.F. & Sharpton, V.L. (eds.) *Large meteorite impacts and planetary evolution.* Geological Society of America, Special Paper 293, 51-59.

Dallmann, W.K., Gjelberg, J.G., Harland, W.B., Johannessen, E.P., Keilen, H.B., Lønøy, A., Nilsson, I. & Worsley, D. 1999: Upper Palaeozoic lithostratigraphy. *In* Dallmann, W.K. (ed.): *Lithostratigraphic lexicon of Svalbard. Review and recommendations for nomenclature use. Upper Palaeozoic to Quaternary bedrock.* Norsk Polarinstitutt, Tromsø, 25-126.

Dypvik, H. & Eriksen, D.Ø. 1983: Natural radioactivity of clastic sediments and the contributions of U, Th and K. *Journal of Petroleum Geology 5*, 409-416.

Dypvik, H. & Ferrell, R.E. Jr. 1998: Clay mineral alteration associated with a meteorite impact in the marine environment (Barents Sea). *Clay Minerals* 33, 51-64.

Dypvik, H. & Attrep, M. Jr. 1999: Geochemical signals of the late Jurassic, marine Mjølnir impact. *Meteoritics and Planetary Science 34*, 393-406.

Dypvik, H. & Jansa, L. 2003: Sedimentary signatures and processes during marine bolide impacts: a review. *Sedimentary Geology 161*, 308-341.

Dypvik, H., Nagy, J., Eikeland, T.-A., Backer-Owe, K. & Johansen, H. 1991a: Depositional conditions of the Bathonian to Hauterivian Janusfjellet Subgroup, Spitsbergen. *Sedimentary Geology 72*, 55-78.

Dypvik, H., Nagy, J., Eikeland, T.-A., Backer-Owe, K., Andresen, A., Haremo, P., Bjærke, T., Johansen, H. & Elverhøi, A. 1991b: The Janusfjellet Subgroup (Bathonian to Hauterivian) on central Spitsbergen; a revised lithostratigraphy. *Polar Research 9*, 21-43.

Dypvik, H., Gudlaugsson, S.T., Tsikalas, F., Attrep, M. Jr., Ferrell, R.E. Jr., Krinsley, D.H., Mørk, A., Faleide, J.-I. & Nagy, J. 1996: Mjølnir structure: An impact crater in the Barents Sea. *Geology 24*, 779-782.

Dypvik, H., Ferrell, R.E. Jr. & Sandbakken, P.T. 2003: The clay mineralogy of sediments related to the marine Mjølnir impact Crater. *Meteoritics and Planetary Science 38*, 1-14.

Dypvik, H., Burchell, M.J. & Claeys, P. 2004a: Impacts into marine and icy environments. *In* Dypvik, H., Burchell, M. & Claeys, P. (eds.) *Cratering in marine environments and on ice.* Springer Verlag, Heidelberg, 1-20.

Dypvik, H., Sandbakken, P.T., Postma, G. & Mørk, A. 2004b: Post-impact sedimentation in the Mjølnir crater. *Sedimentary Geology 168*, 227-247.

Espitalié, J., Laporte, J.L., Madec, M., Marquis, F., Leplat, P., Paulet, J. & Boutefeu, A. 1977: Méthode rapide de caractérisation des roches mères; de leur potentiel pétrolier et de leur degré d'évolution. *Revue de l'Institut Francais du Pétrole 32*, 23-42.

Fertl, W.H. & Rieke, H.H. 1980: Gamma-ray spectral evaluation techniques identify fractured shale reservoirs and source-rock characteristics. *Journal of Petroleum Technology 31*, 2053-2063.

French, B.M. 1998: *Traces of Catastrophe: A Handbook of Shock-Metamorphic Effects in Terrestrial Meteorite Impact Structures.* LPI Contrib. 954, Lunar and Planetary Institute, Houston, 120 pp.

Gabrielsen, R.H., Færseth, R.B., Jensen, L.N., Kalheim, J.E. & Riis, F. 1990: Structural elements of the Norwegian continental shelf. Part I: The Barents Sea region. *Norwegian Petroleum Directorate Bulletin 6*, 33 pp, 16 pls.

Gersonde, R. & Deutsch, A. 2000: New field of impact research looks to the oceans. *Eos, Transactions, American Geophysical Union 81*, 221, 223 & 228

Grieve, R.A.F. 1987: Terrestrial impact structures. *Annual Review of Earth and Planetary Sciences 15*, 245-270.

Grieve, R.A.F. 1991: Terrestrial impact; the record in the rocks. *Meteoritics 26*, 175-194.

Gudlaugsson, S.T. 1993: Large impact crater in the Barents Sea. *Geology 21*, 291-294.

Johannessen, E.P. & Embry, A.F. 1989: Sequence correlation: Upper Triassic to Lower Jurassic succession, Canadian and Norwegian Arctic. *In* Collinson, J.D. (ed.): *Correlation in Hydrocarbon Exploration.* Norwegian Petroleum Society, Graham & Trotman, 155-170.

Johansen, S.E., Ostisty, B.K., Birkeland, Ø., Federovsky, Y.F., Martirosjan, V.N., Bruun Christensen, O., Cheredeev, S.I., Ignatenko, E.A. & Margulis, L.S. 1992: Hydrocarbon potential in the Barents Sea region: play distribution and potential. In: Vorren, T.O. et al. (eds.): *Arctic Geology and Petroleum Potential.* NPF Special Publication no. 2. Elsevier Scientific Publications, 273-320.

Krajewski, K. P. 2000: Phosphogenic facies and processes in the Triassic of Svalbard. *Studia Geologica Polonica 116*, 7-84.

Larssen, G.B., Elvebakk, G., Henriksen, L.B., Kristensen, S.E., Nilsson, I., Samuelsberg, T.J., Svånå, T.A., Stemmerik, L. & Worsley, D. 2002: *Upper Palaeozoic lithostratigraphy of the Southern Norwegian Barents Sea.* 76 pp. http://www.npd.no/Norsk/Produkter+og+tjenester/Publikasjoner/Oversikt+sokkelpublikasjoner/npd+bulletin.htm

Leith, T.L., Weiss, H.M., Mørk, A., Århus, N., Elvebakk, G., Embry, A.F., Brooks, P.W., Stewart, K.R., Pchelina, T.M., Bro, E.G., Verba, M.L., Danyushevskaya, A. & Borisov, A.V. 1992: Mesozoic hydrocarbon source-rocks of the Arctic region. *In* Vorren, T.O. et al. (eds.): *Arctic Geology and Petroleum Potential.* NPF Special Publication no. 2. Elsevier Scientific Publications, 1-25.

Melosh, H.J. 1989: *Impact Cratering. A Geologic Process.* Oxford University Press, 245 pp.

Mørk, A. & Bjorøy, M. 1984: Mesozoic source rocks on Svalbard. *In* Spencer, A.M. et al. (eds.): *Petroleum Geology of the North European Margin.* Norwegian Petroleum Society, Graham & Trotman, 371-382.

Mørk, A., Knarud, R. & Worsley, D. 1982: Depositional and diagenetic environments of the Triassic and Lower Jurassic succession of Svalbard. *In* Embry, A.F. & Balkwill, H.R. (eds.): *Arctic Geology and Geophysics*. Canadian Society of Petroleum Geologists Memoir 8, 371-398.

Mørk, A., Dallmann, W.K, Dypvik, H., Johannessen, E.P., Larssen, G.B., Nagy, J., Nøttvedt, A., Olaussen, S., Pchelina, T.M. & Worsley, D. 1999: Mesozoic lithostratigraphy. *In* Dallmann, W.K. (ed.): *Lithostratigraphic lexicon of Svalbard. Review and recommendations for nomenclature use. Upper Palaeozoic to Quaternary bedrock*. Norsk Polarinstitutt, Tromsø, 127-214.

Mørk, A., Vigran, J.O., Korchinskaya, M.V., Pchelina, T.M., Fefilova, L.A., Vavilov, M.N. & Weitschat, W. 1992: Triassic rocks in Svalbard, the Arctic Soviet islands and the Barents Shelf: bearing on their correlations. *In* Vorren, T.O. et al. (eds.): *Arctic Geology and Petroleum Potential*. NPF Special Publication no. 2. Elsevier Scientific Publications, 457-479.

Mørk, M.B.E. 1999: Compositional variations and provenance of Triassic sandstones from the Barents Shelf. *Journal of Sedimentary Research 69*, 690-710.

Ormö, J. & Lindström, M. 2000: When a cosmic impact strikes the sea bed. *Geological Magazine 137*, 67-80.

Sandbakken, P.T. 2002: A geological investigation of the Mjølnir crater core (7329/03-U-01), with emphasis on shock metamorphosed quartz. Cand Scient (M.Sc.) Thesis, *University of Oslo*, Oslo, Norway, 142 pp.

Schmoker, J.W. 1981: Determination of organic-matter content of Appalachian Devonian shales from gamma-ray logs. *American Association of Petroleum Geologists Bulletin 65*, 1285-1298.

Shuvalov, V.V. 2002: Displacement of target material due to impact. *Proc. Lunar and Planet. Science Conference* 33th, 1259.

Shuvalov, V.V. & Dypvik, H. 2004: Ejecta formation and crater development of the Mjølnir impact. *Meteoritics and Planetary Science 39*, 467 – 479.

Shuvalov, V., Dypvik, H. & Tsikalas, F. 2002: Numerical simulations of the Mjølnir marine impact crater. *Journal of Geophysical*. Resesearch.107, E7, 10.1029, 1-1 to 1-13.

Smelror, M. & Dypvik, H., in press: Dinoflagellate cyst and prasinophyte biostratigraphy of the Volgian-Ryazanian boundary strata, western Barents Shelf. *Norges geologiske undersøkelse Bulletin*.

Smelror, M., Dypvik, H. & Mørk, A. 2002: Phytoplankton blooms in the Jurassic-Cretaceous boundary beds of the Barents Sea possibly induced by the Mjølnir impact. *In* Buffetaut, E. & Koeberl, C. (eds.): *Geological and Biological Effects of Impact Events*. Impact Studies. Springer Verlag, 69-81.

Smelror, M., Mørk, A., Monteil, E., Rutledge, D. & Leereveld, H. 1998: The Klippfisk Formation – a new lithostratigraphic unit of Lower Cretaceous platform carbonates on the Western Barents Shelf. *Polar Research 17*, 81-202.

Smelror, M., Kelly, R.A., Dypvik, H., Mørk, A., Nagy, J. & Tsikalas, F. 2001: Mjølnir (Barents Sea) meteorite impact ejecta offers a Volgian – Ryazanian boundary marker. *Newsletter on Stratigraphy 38*, 129-140.

Steel, R.J. & Worsley, D. 1984: Svalbard's post-Caledonian strata. An atlas of sedimentational patterns and palaeogeographic evolution. *In* Spencer, A.M. et al. (eds.): *Petroleum Geology of the north European Margin*. Norwegian Petroleum Society. Graham & Trotman Ltd., 109-135.

Supernaw, I.R., Arnold, D.M. & Link, A.J. 1978: Method for the evaluation of the source rock potential of earth formation. *United States Patent No. 4,071,755; January 31, 1978.*

Tsikalas, F., Gudlaugsson, S.T. & Faleide, J.I. 1998a: The anatomy of a buried complex impact structure: the Mjølnir Structure, Barents Sea. *Journal of Geophysical Research 103*, 30469-30484.

Tsikalas, F., Gudlaugsson, S.T. & Faleide, J.I. 1998b: Integrated geophysical, analysis supporting the impact origin of the Mjølnir Structure, Barents Sea. *Tectonophysics 289*, 257-280.

Tsikalas, F., Gudlaugsson, S.T. & Faleide, J.I.1998c: Collapse, infilling, and postimpact deformation at the Mjølnir impact structure, Barents Sea. *Geological Society of America. Bulletin 110*, 537-552.

Tsikalas, F., Gudlaugsson, S.T., Faleide, J.I. & Eldholm, O. 1999: Mjølnir Structure, Barents Sea: a marine impact crater laboratory. *Geological Society of America Special Paper 339*, 193-204.

Tsikalas, F., Faleide, J.-I., Eldholm, O. & Dypvik, H. 2002a: Seismic correlation of the Mjølnir marine impact crater to shallow boreholes. *In* Plado, J. & Pesonen L.J. (eds.): *Impacts in Precambrian Shields*. Springer Verlag, Berlin – Heidelberg, 307 – 321.

Tsikalas, F., Gudlaugsson, S.T., Faleide, J.I. & Eldholm, O. 2002b: The Mjølnir marine impact crater porosity anomaly, *Deep-Sea Research Part II 49*, 1103-1120.

Tsikalas, F. & Faleide, J.I. 2003: Near-field erosional features at the Mjølnir impact crater: the role of marine sedimentary target. *In* Dypvik. H., Burchell, M.J. & Clayes, P. (eds.): *Cratering in Marine environments and on Ice*. Springer Verlag, Berlin-Heidelberg, 39-55.

Tsikalas, F. 2004: Mjølnir crater as a result of an oblique impact: asymmetry evidence constrains impact direction and angle. *In* Henkel, H. & Koeberl, C. (eds): *Impact Tectonism*. Springer Verlag, Berlin-Heidelberg, in press.

Van Veen, P.M., Skjold, L.J., Kristensen, S.E., Rasmussen, A., Gjelberg, J. & Stølan, T. 1992: Triassic sequence stratigraphy in the Barents Sea. *In* Vorren, T.O. et al. (eds.): *Arctic Geology and Petroleum Potential*, Norwegian Petroleum Society (NPF) Special Publication no. 2, Elsevier Scientific Publlications., 515-538.

Vigran, J.O., Mangerud, G., Mørk, A., Bugge, T. & Weitschat, W. 1998: Biostratigraphy and sequence stratigraphy of the Lower and Middle Triassic deposits from the Svalis Dome, Central Barents Sea, Norway. *Palynology 22*, 89-141.

Worsley, D., Johansen, R. & Kristensen, S.E. 1988: The Mesozoic and Cenozoic succession of Tromsøflaket. *In* Dalland, A.,Worsley, D. & Ofstad, K. (eds.): A lithostratigraphic scheme for the Mesozoic and Cenozoic succession offshore mid- and northern Norway. *Norwegian Petroleum Directorate Bulletin 4*, 42-65.

Zakharov, V.A., Lapukhov, A.S. & Shenfil, O.V. 1993: Iridium anomaly of Jurassic-Cretaceous boundary Northern Siberia. *Russian Journal Geology and Geophysics 34*, 83-90.